

2019

TRPM7 channels as a bioassay of internal and external Mg²⁺

Charles T. Luu
Wright State University

Follow this and additional works at: https://corescholar.libraries.wright.edu/etd_all



Part of the [Neuroscience and Neurobiology Commons](#), and the [Physiology Commons](#)

Repository Citation

Luu, Charles T., "TRPM7 channels as a bioassay of internal and external Mg²⁺" (2019). *Browse all Theses and Dissertations*. 2252.

https://corescholar.libraries.wright.edu/etd_all/2252

This Thesis is brought to you for free and open access by the Theses and Dissertations at CORE Scholar. It has been accepted for inclusion in Browse all Theses and Dissertations by an authorized administrator of CORE Scholar. For more information, please contact library-corescholar@wright.edu.

TRPM7 channels as a bioassay of internal and external Mg^{2+}

A thesis submitted in partial fulfillment of the
requirements for the degree of
Master of Science

by

CHARLES T. LUU
B.S., Ohio University, 2014

2019
Wright State University

WRIGHT STATE UNIVERSITY
GRADUATE SCHOOL

September 25th, 2019

I HEREBY RECOMMEND THAT THE THESIS PREPARED UNDER MY SUPERVISION BY Charles T. Luu ENTITLED TRPM7 channels as a bioassay of internal and external Mg²⁺ BE ACCEPTED IN PARTIAL FULFILLMENT OF THE REQUIREMENTS FOR THE DEGREE OF Master of Science.

J. Ashot Kozak, Ph.D.
Thesis Director

Eric Bennett, Ph.D
Chair, Department of
Neuroscience, Cell Biology and
Physiology

Committee on Final Examination:

J. Ashot Kozak, Ph.D

Mauricio Di Fulvio, Ph.D.

Kathrin L. Engisch, Ph.D

Barry Milligan, Ph.D.
Interim Dean of the Graduate School

ABSTRACT

Luu, Charles.T. M.S., Department of Neuroscience, Cell Biology and Physiology, Wright State University, 2019. TRPM7 as a bioassay of internal and external Mg^{2+} .

Magnesium is an important divalent metal cation that is involved in numerous cellular functions. The details of cellular Mg^{2+} regulation, homeostasis and transport remain unclear. Magnesium transporter protein (MagT1) is a Mg^{2+} transporter and deficiency of this protein has been reported to lead to impaired Mg^{2+} influx and a decreased cytoplasmic $[Mg^{2+}]$. Transient receptor potential melastatin 7 (TRPM7) is a ubiquitously expressed membrane protein containing a channel pore and a C-terminal alpha-type serine/threonine protein kinase domain. Importantly, TRPM7 channel is believed to conduct both Mg^{2+} and Ca^{2+} . In the present study, we investigated if TRPM7 can be used as a bioassay of internal and external Mg^{2+} in Jurkat T cells. We have investigated the long term effects of Mg^{2+} changes on TRPM7 channel activity. Under physiological conditions, cytoplasmic Mg^{2+} concentrations of 0.1 – 0.3 mM are sufficient to inhibit the majority of TRPM7 channels. Extracellular Mg^{2+} blocks inward TRPM7 currents carried by monovalent cations. When the cytoplasmic Mg^{2+} concentration is reduced, TRPM7 channels open and produce an outwardly-rectifying current. We find that the extent of TRPM7 current activation can be used effectively to estimate changes of cytoplasmic Mg^{2+} concentration. Our findings can be extended to cell types other than Jurkat T cells.

TABLE OF CONTENTS

I.	INTRODUCTION	1
	1.1 Background.....	1
	1.1.1 Ion channels in lymphocytes.....	1
	1.1.2 TRP Channels.....	3
	1.1.3 Magnesium transporter.....	13
	1.1.4 Calcium signaling.....	15
	1.1.5 T-cell receptors.....	19
	1.1.6 Sodium-magnesium antiporter.....	21
	1.2 Significance of TRPM7 and magnesium ion.....	22
	1.3 Medical Importance.....	25
	1.3.1 <u>X</u> -linked immunodeficiency with <u>m</u> agnesium defect, <u>E</u> pstein-Barr Virus (EBV) infection, and <u>n</u> eoplasia (XMEN) disease..	25
	1.3.2 Disturbances of blood magnesium.....	27
	1.4 Hypothesis and Specific aims.....	31
II.	Materials & Methods.....	32
	2.1 Materials.....	32
	2.1.1 Fura-2 AM.....	32
	2.1.2 Cyclopiazonic Acid.....	33
	2.1.3 Ionomycin.....	33
	2.1.4 Ethylene glycol tetraacetic acid.....	34

2.1.5	Amphotericin B.....	34
2.1.6	Amiloride.....	35
2.1.7	Jurkat T cells.....	35
2.1.8	Chelex-RPMI medium.....	36
2.2	Methods.....	36
2.2.1	Maintenance of Jurkat cell line.....	36
2.2.2	Patch-clamp electrophysiology.....	36
2.2.3	Intracellular Ca ²⁺ imaging.....	41
2.2.4	Vi-Cell viability analyzer.....	45
2.2.5	Osmolality of solutions.....	45
2.2.6	Data Analysis.....	46
III.	Results.....	47
3.1	Endogenous TRPM7 channels of Jurkat T cells can be used as a bioassay of external Mg ²⁺ concentration.....	47
3.2	MagT1 knock-out (KO) Jurkat T cells have lower internal concentrations of Mg ²⁺ as determined by TRPM7 channel activity.....	58
IV.	Discussion.....	66
V.	Conclusion.....	70
VI.	References.....	71

List of Figures

Figure 1: Illustration of ion channels in T cells.....	2
Figure 2: Whole cell recording of TRPM7 current in Jurkat T cells.....	7
Figure 3: Potassium and TRPM channels in T cell calcium signaling.....	12
Figure 4: Role of MagT1 during TCR stimulation.....	14
Figure 5: Ca ²⁺ and Mg ²⁺ signaling pathways and store-operated Ca ²⁺ entry.....	18
Figure 6: Patch clamp configurations.....	40
Figure 7: TRPM7 channel activity during Mg ⁺ loading and depletion.....	49
Figure 8: Extracellular Mg ²⁺ does-response relation.....	51
Figure 9: Proliferation of WT and kinase-dead (KD) mouse T cell at increasing external Mg ²⁺ concentrations.....	52
Figure 10: Amiloride sensitivity of TRPM7 currents.....	55
Figure 11: Amiloride sensitivity of Mg ²⁺ efflux and influx in Jurkat T cells.....	56
Figure 12: I-V & time dependence of TRPM7 current in Mg ²⁺ -depleted Jurkat T cells....	57
Figure 13: Viability and diameters of Jurkat cells grown in chelex RPMI supplemented with Mg ²⁺ for 96 hours.....	59
Figure 14: I-V relations using K ⁺ -based solutions in WT and MagT1 KO Jurkat cells....	60
Figure 15: Ca ²⁺ imaging in WT and MagT1 KO Jurkat T cells.....	62
Figure 16: Store-operated CRAC currents in WT and MagT1 KO Jurkat T cells.....	63
Figure 17: Bar graphs of CRAC amplitudes in WT and MagT1 KO Jurkat cells.....	63
Figure 18: TRPM7 I-V relations of WT and MagT1 KO Jurkat T cells.....	65

List of tables:

Table 1: TRPM7 role during early stage development.....24

Table 2: Ca²⁺ Imaging perfusion solution.....44

Abbreviations

CPA - cyclopiazonic acid

CRAC channel - calcium release-activated calcium channel

CID - combined immune deficiency

DAG - diacylglycerol

ER - endoplasmic reticulum

EGTA - ethylene glycol tetraacetic acid

EBV - Epstein-Barr virus

IP₃ - inositol 1,4,5-triphosphate

IP₃R - IP₃ receptors

ITAM - Immunoreceptor tyrosine-based activation motif

LAT - Linker of Activated T cells

Lck - lymphocyte-specific protein tyrosine kinase

MagT1 - magnesium transporter protein 1

NFAT - nuclear factor of activated T-cells

NK - natural killer cells

PI3K - phosphatidylinositol 3-kinase

PIP₂ - phosphatidylinositol 4,5-bisphosphate

PLC - phospholipase C

PMCA - plasma membrane Ca²⁺-ATPase

SERCA - sarco-endoplasmic reticulum Ca²⁺-ATPase

SOCE - store-operated Ca^{2+} entry

STIM - stromal interaction molecule

TCR - T cell receptor

TRPM7 - transient receptor potential cation channel, melastatin subfamily member 7

TUSC3 - tumor suppressor candidate 3

XMEN - X-linked immunodeficiency with magnesium defect, Epstein-Barr virus
infection and neoplasia

Acknowledgements

I would like to first thank my thesis director and mentor, J.Ashot Kozak for allowing me to join his lab. I truly appreciate his guidance, teaching and support during my time as a graduate student. Without Dr. Kozak's assistance, I would have been unable to accomplish my research. In addition, I have to thank my committee members, Drs. Di Fulvio and Englisch for their feedback and comments which have helped me improve my writing.

Also I would like to thank my current and former lab mates Pavani Beesetty, Ngocminh L. Truong, Krystyna B. Wiczerzak, Tatyana Zhelay, Jananie Rockwood, Alayna Mellott, Kalina Szteyn for teaching, helping and assisting me. I will remember fondly the times we spent together in the lab.

A massive thank you to the Department of Neuroscience, Cell Biology and Physiology at Wright State University for accepting me into the program and providing a wonderful learning environment. I thank my friends and family for their support.

Finally a special thanks to Drs. Michael Lenardo and Juan Ravell (NIAID) for the gift of wildtype and MagT1 knockout Jurkat T cell lines.

Reprinted by permission from Springer Nature, Nature Reviews Immunology, Calcium signaling in T cells, Mohamed Trebak, January 2019.

Reprinted by permission from John Wiley and Sons, Immunological Reviews, The functional network of ion channels in T lymphocytes, K. George Chandy, Michael D. Cahalan, September 2009.

Reprinted by permission from Elsevier, *Current Opinion in Immunology*, Ion channelopathies of the immune system, Martin Vaeth, Stefan Feske, June 2018

Reprinted from *Pharmacology*, Georgi V. Petkov, Pages 384-427, 2009, with permission from Elsevier.

Introduction

Magnesium is an essential divalent cation that has numerous roles in cellular functions such as signaling pathways, enzymatic functions, ion channels, metabolic cycles, DNA transcription, protein synthesis, proliferation and preventing cell death (Romani, 2011). The majority of cellular magnesium is bound to nucleic acids, nucleotides, chromatin, proteins, ATP and phospholipids (Romani, 2011). The amount of free cytosolic $[Mg^{2+}]$ is around 0.5 to 1 mM or approximately 5 % of the total concentration of Mg^{2+} in the cell (Feske et al., 2015; F. Y. Li et al., 2011; Romani, 2011). The details of magnesium regulation, homeostasis and transport remain a mystery. Recent studies suggest that magnesium has a more important role in cell signaling than previously appreciated.

Activation of the T-cell receptor (TCR) will activate Magnesium transporter 1 (MagT1) to induce transient Mg^{2+} influx. Loss-of-function mutations in MagT1 cause a decrease in the free intracellular Mg^{2+} concentration. By taking advantage of TRPM7 unique ability to become inhibited or activated depending on the intracellular Mg^{2+} concentration, TRPM7 can be used as a bioassay for Mg^{2+} in Jurkat T cells.

1.1 Background

1.1.1 Ion channels in lymphocytes

Cells of the innate and adaptive immunity express a variety of ion channels and transporters that function to allow the influx and efflux of ions across the plasma membrane and organellar membranes as shown in Figure 1 (Feske et al., 2015). Unlike

excitable cells (e.g neurons), cells of the immune system (e.g lymphocytes and macrophages) do not express significant levels of voltage-gated Na^+ channels. The difference in the electrochemical gradients give rise to the driving force for the passive movement of ions. In addition, energy can be used to transport ions against their concentration gradient primarily using ATP as the energy source.

Ion channels and transporters in lymphocytes are regulated by the membrane potential and cellular signaling (Figure 1). The membrane potential is generally regulated by monovalent cations, such as K^+ , which mediates secondary regulation of influx of calcium in immune cell signaling (Hou et al., 2014). Divalent cations, on the other hand, have a role in the regulation of intracellular signaling pathways.

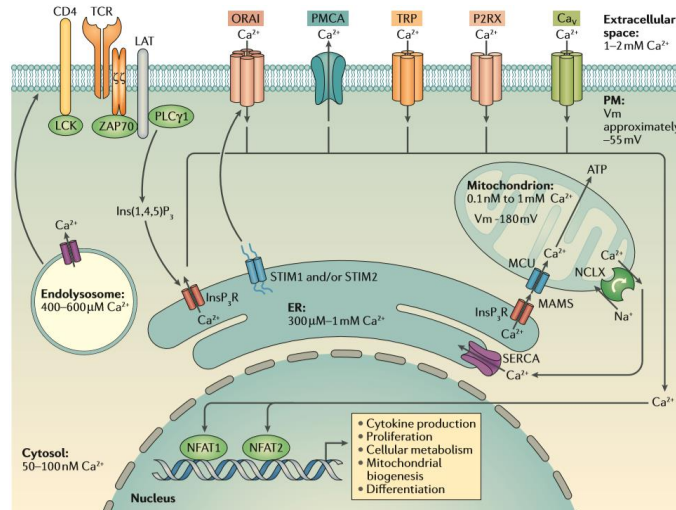


Figure 1: Illustration of ion channels in T-cells

Ion channels, transporters and receptors of the T-cell and estimated concentrations of Ca^{2+} in various compartments (Reproduced from Trebak and Kinet, 2019 with permission).

1.1.2 TRP Channels

Transient Receptor Potential (TRP) channels are members of a large family of ion channels that are located in the plasma membrane and organellar membranes of a variety of animal cells and respond to a wide variety of environmental and intracellular stimuli. TRP proteins are subdivided into 7 subgroups based on their primary sequences (TRPA, TRPC, TRPL, TRPM, TRPN, TRPP and TRPV). TRP channels function in controlling the movement of cations down their electrochemical gradient, which will cause an increase in intracellular concentrations of these cations and in some instances also depolarize the cell (Khalil et al., 2018; Ramsey et al., 2006). The membrane potential determines the driving force for cation entry into the cell and also the gating of voltage-dependent channels. The influx of Ca^{2+} can be a cellular signaling event. The increase in intracellular Ca^{2+} concentration can cause effector proteins to begin a series of cellular events such as transcription, proliferation and migration (Khalil et al., 2018; Ramsey et al., 2006). Multiple stimuli within the tissues are able to activate TRP channels. Examples of activators are G protein-coupled receptors (GPCRs), ligand-gated ion channels (LGIC) and direct activation by other mechanisms. (Ramsey et al., 2006). The main TRP channel in regards to this study, Transient receptor potential cation channel, subfamily M, member 7 (TRPM7), is ubiquitously expressed. Transient receptor potential cation channel, subfamily M, member 6 (TRPM6) is selectively expressed in the intestine and kidneys (Ramsey et al., 2006; Rude, Gruber, Wei, Frausto, & Mills, 2003;

Swaminathan, 2003; Visser, Middelbeek, van Leeuwen, & Jalink, 2014; Voets et al., 2004; Walder et al., 2002).

TRPM6 and TRPM7 are tetrameric channels composed of a 6 transmembrane segment with the channel pore forming between S5 and S6. TRPM6 and TRPM7 can form functional homotetramers or heterotetramers (Brandao, Deason-Towne, Zhao, Perraud, & Schmitz, 2014; Brauchi, Krapivinsky, Krapivinsky, & Clapham, 2008; Cabezas-Bratesco et al., 2015; M. Li, Jiang, & Yue, 2006). However, some studies strongly suggest the formation of functional TRPM6 channels in the cytoplasmic membrane could require coassembly with TRPM7 (M. Li et al., 2006; Ramsey et al., 2006; Venkatachalam & Montell, 2007). On the cytoplasmic side of the plasma membrane, the kinase domain forms homo-dimers (M. Li et al., 2006; Yamaguchi, Matsushita, Nairn, & Kuriyan, 2001). The transmembrane segment is covalently linked to an alpha-type serine/threonine protein kinase domain located at the cytoplasmic C terminus. The kinase domain is a member of the eukaryotic elongation factor 2-kinase (eEF2-K) family and has structural homology with the zinc finger domain of other protein kinases (Middelbeek, Clark, Venselaar, Huynen, & van Leeuwen, 2010; Ryazanov, 2002). The alpha type kinase has the ability to phosphorylate the serine/threonine residues of TRP channels and other proteins such as annexin A1, myosins, eEF2-K, PLC γ 2, tropomodulin and CREB. The kinase could have a role in subcellular localization, channel formation and structure (Cabezas-Bratesco et al., 2015; Clark et al., 2008; Deason-Towne, Perraud, & Schmitz, 2012; Dorovkov, Beznosov, Shah,

Kotlianskaia, & Kostiukova, 2008; M. Li et al., 2006; Matsushita et al., 2005; Ogata et al., 2017; Perraud, Zhao, Ryazanov, & Schmitz, 2011; Ramsey et al., 2006; Venkatachalam & Montell, 2007).

TRP domain consists of highly conserved ~20 amino acid residues found in all known TRP channels and is located next to S6 and the C-terminus (Ramsey et al., 2006; Venkatachalam & Montell, 2007). The TRP domain has been proposed to interact with PI(4,5)P₂ for the regulation of the channel activity. The current understanding of PIP₂ is that it has the ability to stimulate certain TRP channels and inhibit other TRP channels. However, the reason why certain channels are stimulated or inhibited remains uncertain (Ramsey et al., 2006; Rohacs, Lopes, Michailidis, & Logothetis, 2005; Xie et al., 2011). TRPM7 is stimulated by PIP₂ (Zhelay et al., 2018). PIP₂ is hydrolyzed upon ligand-TCR binding and may have an influence on TRPM7 stimulation.

TRPM 6 and 7 contain a non-selective cation channel portion that is able to conduct various divalent cations such as Zn²⁺, Ca²⁺, Ni²⁺, Mg²⁺, Ba²⁺, Sr²⁺, Cd²⁺. There are some differences in the permeability between channels. TRPM6 and TRPM6/7 heterotramers are least permeable to Ni²⁺ whereas Ni²⁺ is one of the most permeable divalent cations for TRPM7 channels (Cabezas-Bratesco et al., 2015; M. Li et al., 2006; Monteilh-Zoller et al., 2003; Ramsey et al., 2006; Venkatachalam & Montell, 2007; Voets et al., 2004). TRPM7 channel is also permeable to monovalent cations like Na⁺, K⁺, and H⁺. TRPM7 allows these monovalent cations to enter the cell in the absence of external divalent cations (Kozak, Kerschbaum, & Cahalan, 2002; Numata & Okada,

2008; Runnels, Yue, & Clapham, 2002). The ion channel has an outwardly-rectifying current-voltage relation in the presence of extracellular divalent cations as shown in Figure 2. Extracellular divalent cations are able to block the channel pore, thus reducing monovalent cation influx. In the presence of extracellular divalent cations, whole cell patch-clamp of TRPM7 shows a steeply outwardly-rectifying current. By contrast, without extracellular divalent cations, TRPM7 and TRPM6 currents are semi-linear. TRPM7 currents can be identified by using intracellular Mg^{2+} chelators (Ramsey et al., 2006). Chelators are substances that have a high affinity to metal ions. Intracellular Mg^{2+} chelators will bind Mg^{2+} and decrease the intracellular concentration of Mg^{2+} , allowing TRPM7 channels to open and produce a current. (Ramsey et al., 2006). The ionic interactions within the channel pore could explain the shape of the steady state TRPM current-voltage relations (Chokshi, Matsushita, & Kozak, 2012b; Kozak, Matsushita, Nairn, & Cahalan, 2005; Ramsey et al., 2006). The channel does not require the kinase domain to function (Faouzi, Kilch, Horgen, Fleig, & Penner, 2017; Matsushita et al., 2005).

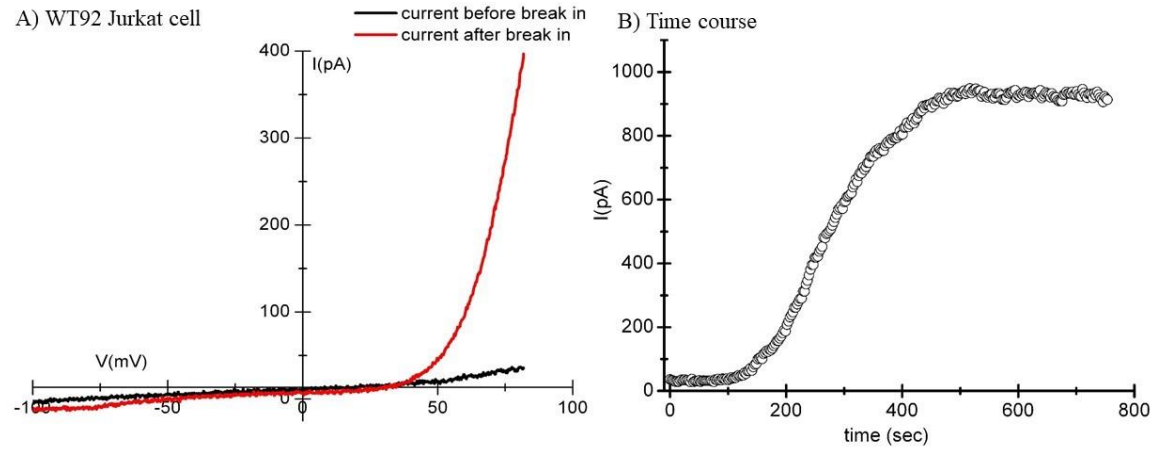


Figure 2: Whole-cell recording of TRPM7 current in a Jurkat T-cell.

2A shows I-V relations of TRPM7 current in Jurkat T-cells. The black trace is the initial current upon rupturing the membrane (break-in). The red trace is the current developed after cytoplasmic Mg^{2+} depletion. 2B: the time course of TRPM7 current development in the same cell as 2A.

Both TRPM6 and TRPM7 have been suggested to have a role in cellular Mg^{2+} uptake (Figure 3). A unique feature of TRPM6 and TRPM7 is that they can be inhibited by low millimolar concentrations of internal Mg^{2+} (0.3-1 mM free) (Ramsey et al., 2006). A substitution of the serine residue bordering the TRP domain makes the channel constitutively active and largely insensitive to intracellular Mg^{2+} concentrations (Hofmann et al., 2014; Zhelay et al., 2018). In the presence of extracellular polyvalent cations, polyamines and protons, the channels can become inhibited through a mechanism that will block the pore via voltage-dependent blockage. There are non-voltage dependent mechanisms that can inhibit the channels as well. Intracellular Mg^{2+} , protons and various polyamines inhibit by electrostatic screening of negative charges of PIP_2 (Chokshi, Matsushita, & Kozak, 2012a; Kozak et al., 2002; Kozak & Cahalan, 2003; Kozak et al., 2005; Zhelay et al., 2018). The majority of the time, TRPM7 channel is inhibited in physiological conditions.

A variety of ions have different effects on TRPM7 channel and the kinase portion. TRPM7 channel activity becomes inhibited by Mg^{2+} while Mg^{2+} will increase the activity of TRPM7 kinase domain, suggesting that the TRPM7 channel portion and TRPM7 kinase domain function in different conditions and cellular activities. The channel is also inhibited by intracellular Ca^{2+} , however Ca^{2+} does not affect TRPM7 kinase activity (Matsushita et al., 2005). Under certain conditions, TRPM7 kinase domain can be cleaved from the TRPM7 channel domain, allowing the TRPM7 kinase domain to translocate into the nucleus to phosphorylate histones and regulate gene expression

(Krapivinsky, Krapivinsky, Manasian, & Clapham, 2014). In T cells, the TRPM7 kinase domain can undergo a caspase-mediated cleavage in response to Fas receptor induced apoptosis. The TRPM7 kinase domain is released from the TRPM7 channel and the truncated TRPM7 was found to have increased channel activity (Desai et al., 2012). Deletion of the kinase domain leads to inactivation of the channel, likely due to problems in the tetramerization and folding (Matsushita et al., 2005).

Currently there are several different mechanisms proposed for the regulation of the TRPM7 channel gating. The changes in intracellular Mg^{2+} concentration is one regulatory mechanism. When the concentration of free intracellular Mg^{2+} is around 0.3-0.4 mM, TRPM7 channel activity is inhibited. Under normal physiological conditions, the free intracellular Mg^{2+} concentration is thought to be in the 0.5-1 mM range. Thus, physiological Mg^{2+} concentrations are within the range to inhibit TRPM7 channel activity (Chokshi, Matsushita, & Kozak, 2012a; Matsushita et al., 2005; Sah, Mesirca, Van den Boogert et al., 2013).

Intracellular pH is another regulatory mechanism of TRPM7. TRPM7 channel activity will decrease when intracellular pH becomes acidic or increase when intracellular pH becomes alkaline. The pH influence can be detected even when the free intracellular Mg^{2+} concentration is 0.5-1 mM (Chokshi, Matsushita, & Kozak, 2012a; Kozak et al., 2005). The TRPM7 kinase reaches its optimal activity rate when intracellular pH is around 7.3. Fluctuations from the optimal pH to acidic pH of 4 - 5.6 or alkaline pH of 8.4 - 9 can result in significant reduction of TRPM7 kinase activity (Kozak et al., 2005). On

the other hand, acidic *extracellular* pH of 4 will cause a 10 fold increase and an acidic extracellular pH of 6 have ~ 2 fold increase of TRPM7 currents. Protons will compete with Ca^{2+} and Mg^{2+} for binding sites in the conduction pathway (Jiang, Li, & Yue, 2005), resulting in divalent cations blocking the inward monovalent currents of TRPM7 (Jiang et al., 2005; Macianskiene, Almanaityte, Jekabsone, & Mubagwa, 2017).

PIP_2 appears to have a dual role in TRPM7 regulation (Kozak et al., 2005; Runnels et al., 2002). Ligands that bind to GPCRs activate PLC, which will begin to hydrolyze PIP_2 . Thus, PLC has an influence on the depletion of PIP_2 . The depletion of PIP_2 has been shown to inhibit the TRPM7 channel activity (Runnels et al., 2002). Continuous PIP_2 depletion inhibits both TRPM6 and TRPM7 currents (Xie et al., 2011). One group has found different ligands and subunit of G-proteins to activate TRPM7 channels (Langeslag, Clark, Moolenaar, van Leeuwen, & Jalink, 2007). The overall significance of PIP_2 sensitivity of TRPM7 in cellular function remains unknown.

Mechanical forces were reported to influence TRPM7 channels (Visser et al., 2014). When vesicles containing TRPM7 fused with the plasma membrane, TRPM7 are exposed to fluid flow resulting in an increase TRPM7 currents (Oancea, Wolfe, & Clapham, 2006). Osmotic cell swelling and stretching of the plasma membrane is another method to activate TRPM7 currents (Numata, Shimizu, & Okada, 2007; Wei et al., 2009). However, other experiments have suggested osmotic swelling induced TRPM7 current was caused by the dilution and decrease of intracellular Mg^{2+} concentrations instead of direct mechanical forces (Bessac & Fleig, 2007).

The phosphorylation state of TRPM7 may also have a regulatory role on TRPM7 channel activity (Kim, Shin, Song, Lee, & Park, 2012). There are 46 autophosphorylation sites in TRPM7 primary sequence. However, not all of the possible phosphorylation sites are actually phosphorylated (Clark et al., 2008; Kim et al., 2012; Matsushita et al., 2005). Treating primary vascular smooth muscle cells with bradykinin causes an increase in the amount of phosphorylation of TRPM7 and intracellular Mg^{2+} concentration (Callera et al., 2009). The serine/threonine residues of TRPM7 were phosphorylated by TRPM6 which had an effect on cellular growth (Brandao et al., 2014; Cai, Bai, Nanda, & Runnels, 2017).

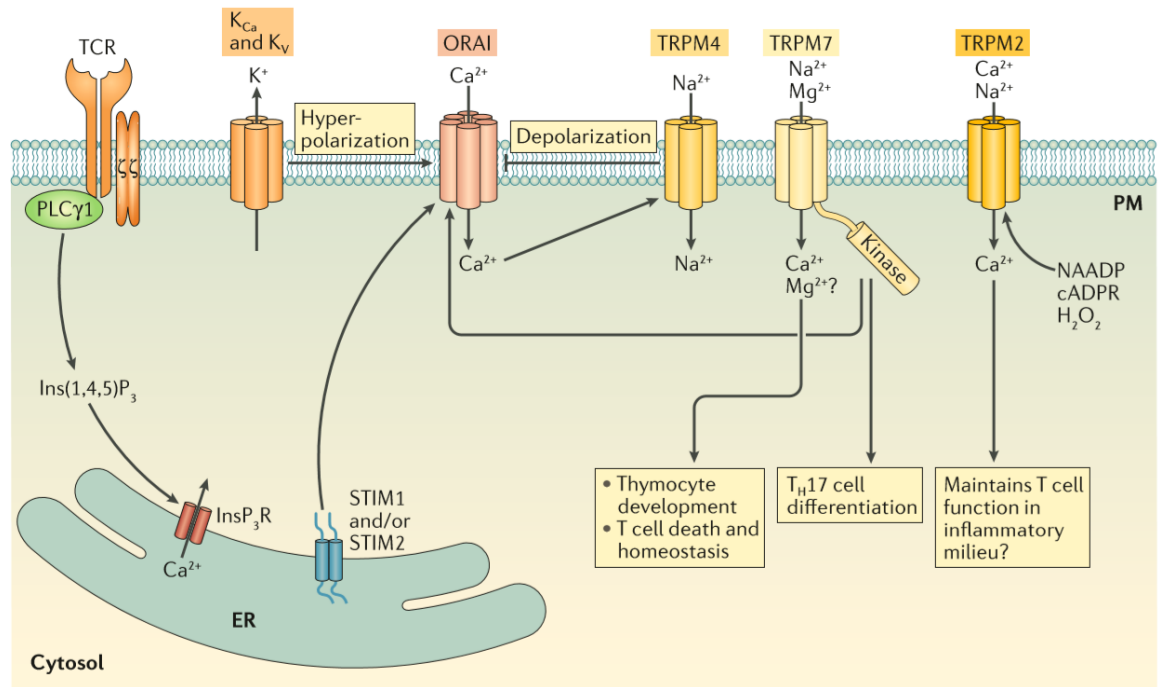


Figure 3: Potassium, Orai and TRPM channels in T-cell calcium signaling.

K⁺ efflux through Ca²⁺-dependent and voltage-dependent K⁺ channels (K_{Ca} and K_V) will cause the membrane to hyperpolarize. Hyperpolarization increases the electrochemical driving force for Ca²⁺ influx through Orai and other Ca²⁺ permeable channels. The kinase domain of TRPM7 is known to regulate SOCE (Reproduced from Trebak and Kinet, 2019 with permission).

1.1.3 Magnesium transport

Mg²⁺ transporter (MagT1) is a highly selective Mg²⁺ transporter that is expressed in all mammalian cells (Figure 4). This membrane protein is 367 amino acid long and contains four transmembrane domains, a long N-terminus and a short C-terminus. MagT1 is located on the X chromosome, at band Xq21.1. Mutations of MagT1 will result in sex-linked diseases. MagT1 is evolutionarily conserved and does not have similarity with other proteins except with tumor suppressor candidate 3 (TUSC3). TUSC3 is a non-selective Mg²⁺ transporter located on chromosome 8p22 and has been associated with Mg²⁺ uptake, glycosylation and development. MagT1 and TUSC3 share a 66% amino acid sequence and both of their genes predict a similar secondary structure. The physiological functions and mechanisms of MagT1 mostly remain unknown. In immune cells, MagT1 and TRPM7 have been shown to have a role in the proliferation and other functions.

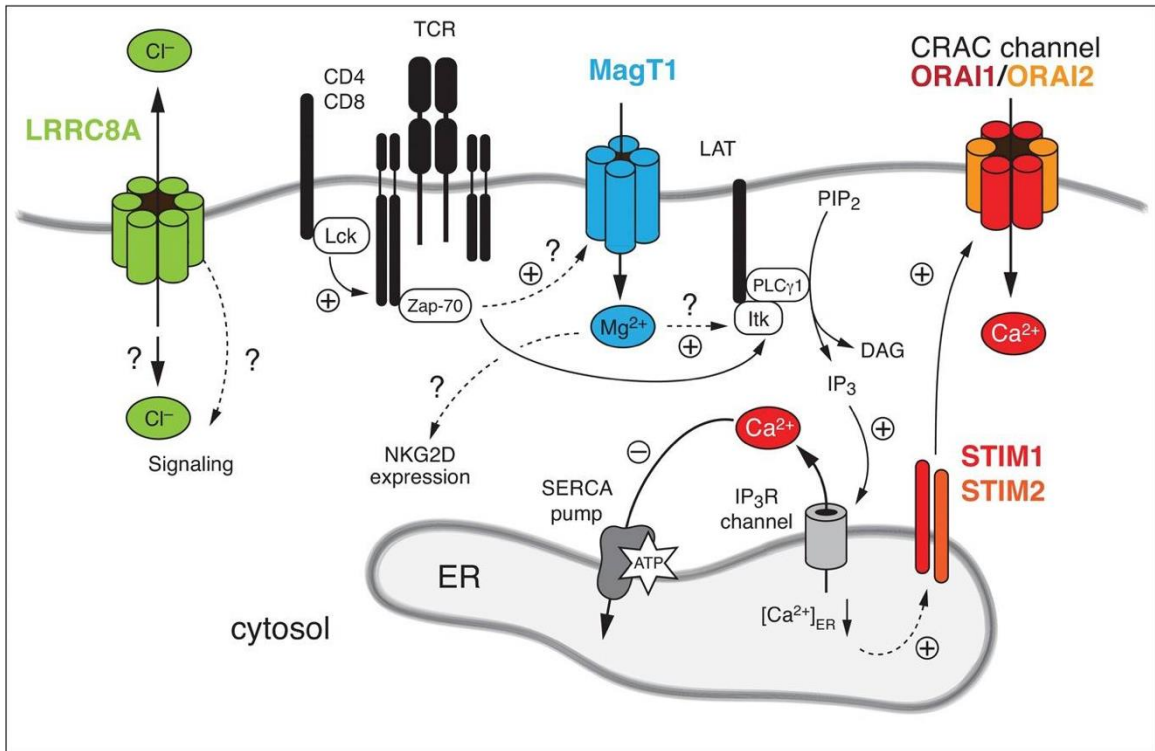


Figure 4: Role of MagT1 during TCR stimulation.

MagT1 is a highly selective Mg^{2+} transporter that is expressed in all mammalian cells. TCR stimulation was reported to activate MagT1 resulting in an influx of Mg^{2+} and increased free intracellular Mg^{2+} concentration and helps activate SOCE, PLC γ and alter NKG2D expression. The physiological mechanism of how TCR activates MagT1 and the role Mg^{2+} has in PLC γ activation remain largely unknown (Reproduced from Vaeth and Feske, 2018 with permission).

1.1.4 Calcium signaling

Calcium ions have an important role in the biological function of various cell types. The role of calcium may range from allosteric regulation of proteins and enzymes, signal transduction from ion channel activation or second messenger in signaling pathways, oscillations of intracellular calcium concentrations, formation of immunological synapse or secretion of hormone-containing vesicles, expression of genes, development, proliferation, apoptosis and migration (Feske et al., 2015; Gwack, Feske, Srikanth, Hogan, & Rao, 2007; Hogan, Lewis, & Rao, 2010; Hogan, 2017; Ramsey et al., 2006). Thus, calcium has critical roles in many functions and key cell controlling factors. In a normal resting cell, the intracellular concentration of calcium is usually 100 nM or lower (Hogan et al., 2010).

The cell is able to maintain intracellular calcium levels due to two types of Ca^{2+} -ATPase enzymes: the plasma membrane Ca^{2+} -ATPase (PMCA) pumps Ca^{2+} out of the cell and the sarco-endoplasmic reticulum Ca^{2+} -ATPase (SERCA) transports Ca^{2+} to be stored in the lumen of the endoplasmic reticulum (ER). In addition, there are several secondary transporters of calcium such as the $\text{Na}^+/\text{Ca}^{2+}$ exchanger (Feske, 2009; Feske et al., 2015; Hogan et al., 2010). The cell regulates intracellular calcium concentrations using various ion channels in the plasma membrane and ER. Ca^{2+} can be released from the ER into the cytoplasm by inositol trisphosphate (IP_3).

Store-operated Ca^{2+} entry (SOCE) is the main pathway of Ca^{2+} influx in human peripheral blood lymphocytes (Figure 5) (Faouzi, Kilch, Horgen, Fleig, & Penner, 2017).

Ca^{2+} is released from the ER store when the T-cell receptor (TCR) or Fc receptor binds to its corresponding ligand (Feske et al., 2015). In Figure 2, the ligand-receptor interaction initiates a signaling cascade which leads to the activation of phospholipase C (PLC) gamma (γ) isoform. Once activated, $\text{PLC}\gamma$ will hydrolyze phosphatidylinositol 4,5-bisphosphate (PIP_2) to produce second messengers 1,4,5-trisphosphate (IP_3) and diacylglycerol (DAG). IP_3 diffuses through the cytosol to bind IP_3 receptors (IP_3R) located in the ER membrane. IP_3R -s are Ca^{2+} -permeable channels gated by IP_3 . The binding of IP_3 and opening of these channels causes ER Ca^{2+} stores to be emptied and the concentration of ER Ca^{2+} drops below the resting values of $\sim 400\text{-}600\ \mu\text{M}$ (Hogan et al., 2010). Depletion of Ca^{2+} from the ER lumen is detected by STIM 1 and 2 proteins. Stromal interaction molecule 1 and 2 (STIM1 & STIM2) are single-pass transmembrane proteins that are primarily localized in the membrane of the ER. (Hogan et al., 2010; Roos et al., 2005). STIM1 and STIM2 function by sensing the depletion of Ca^{2+} in the ER lumen and communicating the ER store Ca^{2+} concentration to plasma membrane Ca^{2+} channels. Upon Ca^{2+} depletion, STIM1 and STIM2 will undergo a conformational change to assemble into oligomers and translocate underneath the cell membrane. Then STIM1 and STIM 2 will directly interact with ORAI1. ORAI1 is a transmembrane protein that assembles to form the pore subunit of CRAC channel (Hogan et al., 2010). STIM1 and STIM2 will bind and activate ORAI1 to form the Ca^{2+} release-activated Ca^{2+} (CRAC) channel, which will allow Ca^{2+} influx through these channels (Feske, 2009; Feske et al., 2015; Hogan et al., 2010).

The influx of Ca^{2+} through CRAC channels will rapidly elevate the concentration of Ca^{2+} in the cytoplasm. The increased intracellular Ca^{2+} will activate calmodulin, causing in turn the activation of the phosphatase calcineurin. Calcineurin will dephosphorylate NFAT which will then be able to translocate to the nucleus where it can bind to DNA (Gwack et al., 2007; Hogan, 2017). NFAT is able to form cooperative transcriptional complexes with a variety of transcription factors to transcribe the genes required for activation and proliferation such as interleukin genes like IL-2 (Gwack et al., 2007; Hogan, 2017; Smith-Garvin, Koretzky, & Jordan, 2009). Thus, during the activation of T cells, there is an increased expression of both STIM1 and ORAI1 (Lioudyno et al., 2008).

K^+ channels promote the continuous influx of Ca^{2+} through CRAC channels by altering the membrane potential through voltage-gated and Ca^{2+} -activated channels $\text{K}_v1.3$ and $\text{K}_{Ca}3.1$ (Figure 3). Calcium entry is promoted by the efflux of potassium through $\text{K}_v1.3$ channels and resulting hyperpolarization (Feske et al., 2015; Gwack et al., 2007; Hou et al., 2014). The membrane hyperpolarization will increase the electrochemical driving force for Ca^{2+} influx through CRAC and other Ca^{2+} permeable channels. In addition to $\text{K}_v1.3$, intracellular Ca^{2+} bound to calmodulin will be able to interact and open $\text{K}_{Ca}3.1$ channels. Overall, the driving force for Ca^{2+} is increased when membrane potential hyperpolarization occurs due to $\text{K}_v1.3$ and $\text{K}_{Ca}3.1$ channels opening, thus maintaining a substantial continuous influx of Ca^{2+} that is required for T cell function (Feske et al., 2015; Hogan et al., 2010; Hou et al., 2014; Pegoraro et al., 2009).

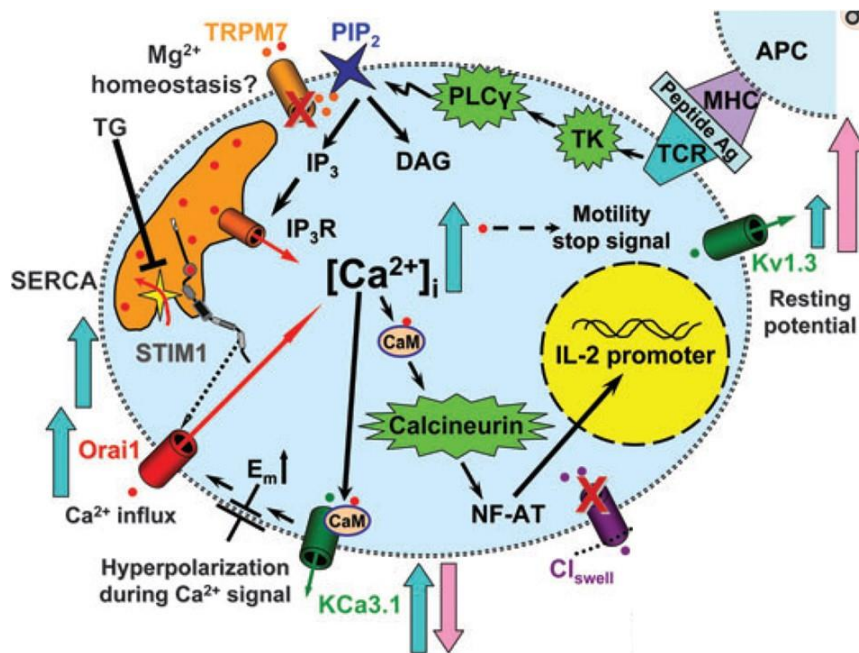


Figure 5: Ca^{2+} and Mg^{2+} signaling pathways and store-operated Ca^{2+} entry

Activation of TCR initiates a signaling cascade resulting in the activation of $\text{PLC}\gamma$, which hydrolyzes PIP_2 to produce second messengers IP_3 and DAG. IP_3 diffuses through the cytosol and binds IP_3R -s located in the ER membrane. IP_3R -s open, allowing ER Ca^{2+} stores to be emptied and simultaneously transiently increasing the cytoplasmic Ca^{2+} concentration. STIM1 detects the depletion of Ca^{2+} from the ER lumen and undergoes a conformational change and translocates to areas close to ORAI1 transmembrane protein. STIM1 interacts with ORAI1 allowing Ca^{2+} influx into the cell. The increased Ca^{2+} concentration in the cytoplasm activates calmodulin, which in turn activates the phosphatase calcineurin. NFAT is dephosphorylated by calcineurin and translocates to the nucleus to promote expression of genes required for T cell activation and proliferation (Reproduced from Cahalan and Chandy, 2009 with permission).

1.1.5 T-cell receptors

CD3 T-cell co-receptor consists of a protein structure composed of CD3 ϵ , CD3 γ and CD3 δ chains. The transmembrane region of the CD3 chains is negatively charged to allow the chains to associate with positively charged TCR. The cytoplasmic tail region contains an ITAM which is a conserved sequence of two tyrosine residues flanking an isoleucine or leucine series of amino acid residues. (Smith-Garvin et al., 2009) TCR ligation by a cognate antigen induces a conformational change in the cytoplasmic tail region, allowing lymphocyte-specific protein tyrosine kinase (lck) to phosphorylate ITAMs (El Hentati, Gruy, Iobagiu, & Lambert, 2010; F. Y. Li et al., 2011; Smith-Garvin et al., 2009). ZAP-70, which is a cytoplasmic tyrosine kinase, will be able to bind, thus allowing lck to phosphorylate and activate ZAP-70. Activated ZAP-70 will then phosphorylate the transmembrane protein, linker of activated T cells (LAT) which functions as a scaffolding protein in the signaling cascade for the activation of PLC and other downstream effectors such as NFAT and NF- κ B (El Hentati et al., 2010; F. Y. Li et al., 2011; Smith-Garvin et al., 2009).

NKG2D is a type 2 transmembrane protein of C-type lectin-like receptors expressed on the surface of all natural killer (NK), all CD8⁺ T cells and subsets of CD4⁺ T cells. NKG2D is encoded by KLRK1 gene which is located within NK-gene complex on chromosome 12 (Lanier, 2015; Raulet, Gasser, Gowen, Deng, & Jung, 2013; Verneris, Karimi, Baker, Jayaswal, & Negrin, 2004). NKG2D receptor complex is stabilized and expressed on the cell surface by associating with DAP10 adapter protein. The receptor is

able to recognize a wide range of induced-self proteins. Upon binding the corresponding ligand, DAP10 will recruit phosphatidylinositol 3-kinase (PI3K) and other signaling adapter proteins (Burgess et al., 2008; Lanier, 2015; Raulet et al., 2013). Different NKG2D ligands will vary considerably in their sequences as well as their affinities (Burgess et al., 2008; Lanier, 2015; Raulet et al., 2013; Wiemann et al., 2005).

Overall, NKG2D signaling is complex and the mechanisms remain unknown. The interaction between NKG2D ligand and NKG2D receptor on resting CD8⁺ T cells and NK cells is insufficient to induce cytokine production and cytotoxicity. In addition to the interaction, NK cells require IL2 and IL15 to begin cytokine production and cytotoxicity. In CD8⁺ T cells, NKG2D functions more as a T-cell costimulatory molecule and is unable to induce Ca²⁺ influx, cytokine production or cytotoxicity in resting CD8⁺ T cells. NKG2D signaling in antigen-activated CD8⁺ T cells will enhance cytotoxicity, cytokine production and proliferation of active CD8⁺ T cells (Burgess et al., 2008; Chaigne-Delalande et al., 2013; Lanier, 2015; Raulet et al., 2013; Verneris et al., 2004; Wiemann et al., 2005).

T cells require both IL-2 and CD3 or CD3/CD28 antibodies for stimulation. CD3 or CD3/CD28 antibodies will promote an increase of cell surface NKG2D. T cells that are exposed to high concentration of IL-2, will express DAP10 for signaling and are able to perform cytolysis. Without DAP10, T cells are unable to perform cytotoxicity. Thus, IL-2 could have a key role in NKG2D-DAP10 signaling pathway regarding activation

and protein expression (Burgess et al., 2008; Chaigne-Delalande et al., 2013; Lanier, 2015; Raulet et al., 2013; Verneris et al., 2004; Wiemann et al., 2005).

In addition, NKG2D expression are reduced in natural killer cells and CD⁸⁺ T cells with nonfunctional MagT1. Without MagT1, the intracellular free Mg²⁺ concentrations are decreased resulting in reduction of NKG2D expressions. When magnesium was supplemented in natural killer cells and CD⁸⁺ T cells with nonfunctional MagT1, the intracellular free Mg²⁺ was restored and NKG2D expressions was increased (Chaigne-Delalande et al., 2013). Suggesting the Mg²⁺ influx of MagT1 has a role in NKG2D expression.

1.1.6 Sodium-magnesium antiporter

Sodium-magnesium antiporter is a type of non-electrogenic transporter that exchange two extracellular Na⁺ for a single intracellular Mg²⁺. The antiporter has been proposed to direct Mg²⁺ efflux from the cell. The extracellular electrochemical concentration gradient of Na⁺ is the main driving force for their movement. Altering the membrane potential could reverse the direction of the exchanger if the sodium gradient was also reversed. Intracellular Mg²⁺ has a strong allosteric effect on Na⁺/Mg²⁺ antiporter causing its activation. Amiloride has an inhibitory effect on Na⁺/Mg²⁺ antiporters at submillimolar concentrations (Gunther, 2006; Long & Romani, 2014; Standley & Standley, 2002).

1.2 Significance of TRPM7 and Mg²⁺

The importance role of TRPM7 in the cell was confirmed by generating TRPM7 knock-out animals. Macrothrombocytopenia was seen in mice with megakaryocyte and platelet TRPM7 knock out (Stritt et al., 2016). If TRPM7 was deleted in the T cell lineage, thymopoiesis was interrupted and T cell development terminated at the double negative stage. An acceleration of thymic involution was also observed (Jin et al., 2008). Mutation in the pore region of TRPM7 in developing T cells interferes with development (F. Y. Li et al., 2011).

In cardiac cells, deletion of TRPM7 before E9 results in congestive heart failure and death. When deletion of TRPM7 occurred between E9 and E11.5, 50% of the mice had cardiomyopathy and arrhythmias. After E13, the mice had normal heart function without any defects (Sah, Mesirca, Mason et al., 2013; Sah, Mesirca, Van den Boogert et al., 2013). TRPM7 deletion in metanephric mesenchymal cells at E11.5 caused defects in nephrogenesis such as smaller kidneys, fewer glomeruli and larger renal cysts. TRPM7 appears to have a role in the development of neural crest during various embryonic stages. In the absence of TRPM7 the neural crest-derived pigment cells are unable to develop. These nonfunctional cells will cause the hind legs to become paralyzed as well as a loss of large-diameter sensory neurons in the lumbar dorsal root ganglion (Jin et al., 2012). The loss of TRPM7 will interrupt melanogenesis, skeletogenesis, nephrogenesis, exocrine pancreatic organogenesis and touch response in zebrafish (Jansen et al., 2016). In *Xenopus*, the gastrulation phase was affected (Yee, Kazi, & Yee, 2014). TRPM7 is

involved in the fusion of cholinergic vesicles with the plasma membrane to release neurotransmitters into the cholinergic synapses for sympathetic neurons (Brauchi et al., 2008; Krapivinsky, Mochida, Krapivinsky, Cibulsky, & Clapham, 2006). It is unknown if TRPM7 kinase domain or the complete TRPM7 mediate these effects, since the complete TRPM7 deletion was lethal.

TRPM7 has a regulator role in cellular magnesium homeostasis (Ryazanova et al., 2010). A deletion was made in the kinase domain of TRPM7. Embryonic stem cells from homozygous TRPM7 kinase dead mice were unable to proliferate and stopped at the G₀ stage of the cell cycle (Romani, 2011; Ryazanova et al., 2010). The cell would normally synthesize molecules in the next stage of the cell cycle and required additional magnesium for binding ATP, RNA, proteins and other molecules. The dysfunctional TRPM7 caused a reduction of the intracellular concentrations of magnesium that was available for binding the newly synthesized molecules thus halting the cell in the G₀ stage (Jin et al., 2008). Mouse heterozygous embryonic stem cells survive, however, these cells had a reduction in TRPM7 channel activity.

Table 1: TRPM7 role during development

Model Organism	TRPM7 Mutation type and in cell type	Effects	References
Mouse	Megakaryocyte & Platelet	Macrothrombocytopenia	Stritt et al., 2016
	T cell lineage	Interrupt thymopoiesis Thymic involution	Jin et al., 2008
	Cardiac cells	Congestive heart failure and death Cardiomyopathy	Sah, Mesirca, Mason et al., 2013 Sah, Mesirca, Van den Boogert et al., 2013
	Metanephric mesenchymal cells	Defects in nephrogenesis	Jin et al., 2008
	Neural crest-derived pigment cells	Impaired development Paralyzed hindlimbs Loss of sensory neurons in lumbar doesal root ganglion	Jin et al., 2008
	Homozygous deletion	Embryonic death between E6.5 - E7.5	Yee, Kazi, & Yee, 2014
Zebrafish	TRPM7 loss of function	Defects in Melanogenesis Defects in Skeletogenesis Defects in Nephrogenesis Defects in Exocrine pancreatic Defects in Organogenesis Defects in Touch response	Jansen et al., 2016
Xenopus	Homozygous deletion	Defects in Gastrulation phase	Yee, Kazi, & Yee, 2014

TRPM7 is highly expressed in T cells. The physiological role of TRPM7 is believed to be involvement with the regulation of lymphocyte proliferation and growth via sustaining the activation of PI3 pathways (Sahni & Scharenberg, 2008; Sahni, Tamura, Sweet, & Scharenberg, 2010). TRPM7 is responsible for fas receptor induced apoptosis in T cells upon constant TCR stimulation. Without TRPM7, T cells would be unable to respond to fas receptor induced apoptosis (Desai et al., 2012). TRPM7 has some unknown physiological mechanism regarding these pathways. It is believed to involve the entry of Ca^{2+} or Mg^{2+} into the cell.

Magnesium may have an influence in the embryonic development. MagT1 and TUSC3 are two gene products that appear to be important mechanisms in Mg^{2+} influx. Without one of these genes, there is a decrease in the concentration of intracellular Mg^{2+} (Zhou & Clapham, 2009). However, when both of these genes are deleted, the mutant cells are unable to survive (Jin et al., 2008; Jin et al., 2012; Zhou & Clapham, 2009).

1.3 Medical Importance

1.3.1 X-linked immunodeficiency with magnesium defect, Epstein-Barr Virus (EBV) infection, and neoplasia (XMEN) disease

XMEN disease has demonstrated that free intracellular magnesium in immune cells has an important role in development, proliferation and activation. X-linked immunodeficiency with magnesium defect, Epstein-Barr Virus (EBV) infection, and neoplasia (XMEN) disease is a rare genetic sex-linked disease that is a form of combined immune deficiency (CID). XMEN is caused by loss-of-function mutations in MagT1

DNA sequence. Due to changes in the DNA sequence, there are several MagT1 mutations. All of the mutations will result in premature translational termination and nonsense-mediated decay of mRNA. XMEN is believed to be phenotypically heterogeneous. XMEN patients have a wide range of ages (3 to 45 years). In addition, the age of exposure to EBV and environmental variables could also have an influence and remains unknown. Since the gene encoding for the transporter is located on the X chromosome, it follows the x-linked inheritance and appears in both males and females as carriers.

XMEN disease is characterized by CD4 lymphopenia, chronic viral infections, decreased expressions of natural killer (NK) cells and CD8⁺ T cells. EBV infections appear to be regulated by intracellular Mg²⁺ in immune cells. Patients with XMEN disease have a lower concentration of free intracellular Mg²⁺ in their NK and CD8⁺ T cells. However, the concentration of bound Mg²⁺ is not altered from the physiological concentration. Therefore, XMEN patients tend to have a higher concentration of EBV, increased EBV infected B-cells, and increased susceptibility to EBV related lymphoproliferative diseases. (Kornreich, 2007; Ran et al., 2013; Ravell, Chaigne-Delalande, & Lenardo, 2014).

The activation of T-cell receptors (TCR) induces influx of Mg²⁺ via MagT1 protein. Mg²⁺ is proposed to increase the efficiency of T-cell activation. With the loss of MagT1, T-cell activation becomes impaired since there is no longer a rapid influx of Mg²⁺, resulting in a delay in the activation of PLCγ1 (F. Y. Li et al., 2011). The

downstream signaling pathways are suggested to be affected resulting in a reduction of IP₃ and DAG generation (Kornreich, 2007; F. Y. Li et al., 2011; Ran et al., 2013; Ravell et al., 2014). The pathway between TCR stimulation, MagT1 induced rapid Mg²⁺ to increase the concentration of free intracellular Mg²⁺ and activation of PLCγ1 remains unknown (Kornreich, 2007; Ran et al., 2013; Ravell et al., 2014). MagT1 could have an upstream role in this pathway mechanism.

Intracellular Mg²⁺ has an effect on NKG2D receptors on NK cells and CD8⁺ T cells. NK and CD8⁺ T cells of XMEN patients have a reduction in the expression of NKG2D receptors. The reduction of expressed NKG2D receptor may why there are high levels of EBV and higher susceptibility to EBV related illness. MagT1 might have a regulation in the basal levels of free intracellular Mg²⁺ in XMEN, which is required to maintain the expression of cytotoxicity activating receptors. Previous studies have shown supplementation of Mg²⁺ is able to restore the basal levels of free intracellular Mg²⁺ in the T-cell of XMEN patients, restoring NKG2D expressions on NK cells and CD8⁺ T cells.

1.3.2 Disturbances of blood magnesium

Magnesium tends to be a forgotten electrolyte until the concentration of blood magnesium falls to an extremely low range and rare symptoms appear. Some studies have indicated that about three-fourth of Americans do not acquire the recommended daily amount of magnesium. The total range for intracellular magnesium is around 10 - 30 mM and free internal magnesium is around 0.5 – 1.2 mM (Ahmed & Mohammed, 2019; Long

& Romani, 2014). Maintaining the normal serum magnesium concentration is the daily intake function of the intestinal and renal ability to take up magnesium. The kidneys filter about 70 % of serum magnesium. A magnesium-deficient diet will cause the serum magnesium to drop to a concentration of around 0.1 – 0.4 mM, and it is called hypomagnesemia. Severe cases of hypomagnesemia have the concentration dropping under 0.05 mM. Overall, the causes of hypomagnesemia have been divided into three categories: increased losses of magnesium from renal or gastrointestinal systems, redistribution of extracellular magnesium to intracellular and an overall decrease in magnesium intake.

Hypomagnesemia can cause a variety of illnesses and diseases ranging from asymptomatic to life-threatening. The lack of magnesium affects neuromuscular and nervous, cardiovascular system, endocrine systems and cellular biochemical functions. (Ahmed & Mohammed, 2019; Swaminathan, 2003). Currently, the clinical and experimental data are contradictory.

Hypomagnesemia could be linked to osteoporosis. The magnesium content in trabecular bone is reduced in osteoporosis patients, however, the connection between low magnesium and osteoporosis remains uncertain (Ahmed & Mohammed, 2019; Long & Romani, 2014; Rude et al., 2003).

Type 2 diabetes patients have been reported to lack magnesium. Around 13 - 48 % of type 2 diabetes patients are hypomagnesemic compared to about 3 - 15% of patients without type 2 diabetes. Magnesium deficiency has an inverse relationship with glycemic

regulation and magnesium deficiency will alter glucose transport, reduce insulin secretion and post-receptor insulin signaling. In addition, indication of hypomagnesemia appears to predict post-transplant development of diabetes in kidney transplant recipients (Ahmed & Mohammed, 2019; Dasgupta, Sarma, & Saikia, 2012; Long & Romani, 2014; Rosanoff, Weaver, & Rude, 2012).

Hypomagnesemia patients tend to also have hypokalemia. Magnesium concentration has to be restored before resolving potassium depletion (Ahmed & Mohammed, 2019). In magnesium deficiency conditions, the hypokalemia can be a secondary effect due to multiple mechanisms. The activity of renal outer medullary potassium (ROMK) channel is regulated by magnesium. ROMK channel is located on the apical surface of the distal tubule and is an inwardly rectifying potassium channel which will conduct potassium outward (Ahmed & Mohammed, 2019; Huang & Kuo, 2007; Long & Romani, 2014). Normally, high intracellular magnesium concentrations will prevent potassium efflux by inhibiting the channels. When the concentration of intracellular magnesium is reduced, ROMK channel will be unblocked and potassium efflux occurs. In addition, there are other mechanisms linked to Na-K ATPase, Na-K cotransporters and other magnesium transport processes (Ahmed & Mohammed, 2019; Ryan, 1993).

Hypomagnesemia with secondary hypocalcemia can develop if the mutations occur in TRPM6 genes (Ramsey et al., 2006; Schlingmann et al., 2002; Swaminathan, 2003; Venkatachalam & Montell, 2007; Viering, de Baaij, Walsh, Kleta, & Bockenhauer,

2017; Walder et al., 2002). Magnesium supplementation therapy is able to resolve hypocalcemia in hypomagnesemia patients. There are several mechanisms that are believed to be involved for hypocalcemia conditions in hypomagnesemia. These range from PTH metabolism, PTH secretion, reduction of vitamin D and organ resistances to PTH (Ahmed & Mohammed, 2019; Long & Romani, 2014; Rude et al., 2003).

Hypermagnesemia is characterized by an increase of serum magnesium above 1.07 mmol/L (Jahnen-Dechent & Ketteler, 2012). It is an uncommon clinical condition and is related to patients with kidney diseases and elderly individuals. In addition, hypermagnesemia is often undiagnosed since magnesium concentration is not measured routinely and the initial symptoms are nonspecific. Hypermagnesemia could result in a wide range of neuromuscular impairment such as hypotonia, areflexia, respiratory dysfunction, drowsiness and coma in extreme conditions. Cardiovascular system is also affected and ranges from atrial fibrillation, asystole, heart blockage, bradycardia and uncharacteristic electrocardiogram.

1.4 Hypothesis and specific aims

Given the importance of magnesium in immune functions; numerous medical issues with magnesium derangement, and the lack of knowledge of magnesium regulation and homeostasis, there is a requirement for a method to monitor magnesium concentrations in living cells.

Hypothesis: TRPM7 can be used as a bioassay for Mg^{2+} in Jurkat T cells.

Specific aims:

1. Determine if endogenous TRPM7 current can act as a bioassay for external Mg^{2+}
2. Test if the internal concentration of Mg^{2+} is lowered when MagT1 is knocked out by using TRPM7 channel activity as a readout.

II. Materials and Methods

2.1 Materials

2.1.1 Fura-2 AM

Fura-2-acetoxymethyl ester (Fura 2-AM) is a ratiometric calcium indicator used in intracellular calcium imaging. It has a distinct fluorescence spectrum when calcium is bound vs. not bound. The acetoxymethyl ester converts Fura-2 into a lipophilic molecule and allows Fura 2-AM to diffuse across the cell membrane. Cytosolic esterases cleave the –COOH groups off Fura 2-AM, regaining the negative charge of Fura-2 (Paredes, Etzler, Watts, Zheng, & Lechleiter, 2008). Esterification allows Fura-2 to bind Ca^{2+} and also prevent charged Fura-2 from diffusing across the cell membrane.

When calcium concentration is low, most Fura 2-AM molecules do not bind calcium and the excitation peak is around 370 nm. The excitation peak of Fura 2-AM changes to about 340 nm when there is a high concentration of free calcium. When Fura 2 binds to calcium and is excited there is an increase in the fluorescence at 510 nm. The process is monitored at ~510 nm and both wavelengths are excited in a rapid succession to allow the observation of the change in Fura 2-AM binding to calcium. The ratio of the two wavelengths allows the values to be normalized to provide an accurate measurement of the intracellular concentration of calcium. Importantly, ratiometric dyes also account for unequal loading of cells.

2.1.2 Cyclopiazonic Acid

Cyclopiazonic acid (CPA) is an inhibitor of sarco-endoplasmic reticulum calcium transport ATPase (SERCA). Since CPA has a high affinity for SERCA, it has been demonstrated to primarily affect SERCA in cells (Laursen et al., 2009). CPA functions to inhibit SERCA by inducing the emptying of ER Ca^{2+} stores. In the presence of CPA, the concentration of cytoplasmic calcium will continue to increase as the ER Ca^{2+} stores are depleted. A Ca^{2+} -free external solution with an added Ca^{2+} chelator (i.e. EGTA) is used with CPA for superfusion. Since CPA is membrane- permeable, the inhibition of SERCA by CPA occurs quickly after adding the drug (several seconds). After several minutes, a Ca^{2+} containing solution is superfused. By using CPA first, ER Ca^{2+} stores are depleted. Any resulting increase in the concentration of intracellular calcium in presence of extracellular Ca^{2+} is therefore due to influx of calcium entering the cell from the external solution. The Ca^{2+} influx can be identified using this method.

2.1.3 Ionomycin

Ionomycin is a type of lipid-soluble ionophore that is capable of reversibly binding ions. It is able to function as an ion carrier to rapidly transport divalent cations across the cell membranes. Ionomycin is highly specific for Ca^{2+} . In addition, ionomycin is able to transport Ca^{2+} in a one to one stoichiometry thus making ionomycin an effective Ca^{2+} ionophore (Liu & Hermann, 1978). Ionomycin is perfused at the end of intracellular calcium imaging as a dye loading control.

2.1.4 Ethylene glycol tetraacetic acid (EGTA)

Ethylene glycol tetraacetic acid (EGTA) is a cation chelator that has a higher affinity towards Ca^{2+} than other common biological cations such as Na^+ , K^+ and Mg^{2+} . EGTA is used in the external solutions to bind any free Ca^{2+} and in less proportion other divalent cations to prevent it entering the cell. In external solutions containing EGTA any observed increase in concentration of internal calcium would be due to the intracellular store Ca^{2+} release.

2.1.5 Amphotericin B

Amphotericin B is an antifungal antibiotic and functions by forming ion channels in the plasma membrane. When the plasma membrane is exposed to amphotericin B, it inserts itself into the lipid portion of membrane and self-assembles into an ion channel that traverses the membrane. The ion channels created by amphotericin B, then allow ions to leak across the membrane resulting in the reduction of the membrane electrical resistance. Amphotericin is often used in electrophysiology for perforated patch recording, where amphotericin channels formed in plasma membrane are used to establish electrical connection with cell interior. This approach is useful for keeping cytosolic Mg^{2+} and Ca^{2+} intact since amphotericin channels do not conduct divalent cations (Kiryakova, Dencheva-Zarkova, & Genova, 2014).

2.1.6 Amiloride

Amiloride is a drug that affects the cellular pH by inhibiting sodium-hydrogen exchangers (NHE1-3) (Frelin et al., 1988; Masereel, Pochet, & Laeckmann, 2003). It is also a known inhibitor of Na^+ - Mg^{2+} transporter.

2.1.7 Jurkat T cells

Jurkat cells are an immortalized cell line generated from leukemic human T-lymphocytes. They are widely used to study T-cell signaling (Abraham & Weiss, 2004; Imboden, Weiss, & Stobo, 1985). Jurkat cell lines used were from ATCC and two cell lines were provided by NIH called WT92 and J1022 lines. Both the Jurkat ATCC and Jurkat WT92 are wild type cell lines and the only difference is the supplier. The J1022 Jurkat cell line has a point mutation in its magnesium transporter protein 1 (MagT1) resulting in a nonfunctional protein.

The J1022 Jurkat cell line was created from the WT92 Jurkat cell line by using CRISPR-Cas system, which is an accurate genetic modification tool. Cas endonuclease uses a synthetically created guide RNA to combine with Cas endonuclease. The guide RNA will direct the Cas endonuclease to vicinity of the desire DNA sequence to allow editing of the target DNA sequence (Kornreich, 2007; Ran et al., 2013). The MagT1 KO and WT92 Jurkat cell lines were created and provided by Dr. Michael Lenardo, NIAID, National Institutes of Health, Bethesda, MD.

2.1.8 Chelex-RPMI

Chelex is a chelating material that is used to bind and remove transition metal ions in RPMI-1640 medium. After removing the transition metal ions, the RPMI could be supplemented with different concentrations of Mg^{2+} and Ca^{2+} . Chelex RPMI was produced using RPMI-1640, 25 mM HEPES, 45 mL of heat inactivated FBS, 5 ml of 100x P/S and 5% chelex 100 sodium. 5 grams of chelex 100 sodium form was added to the RPMI-1640 with 25 mM HEPES, 10 % FBS and 100x P/S. The solution was stirred at room temperature for 1.5 hrs. Afterwards, the solution was filter-sterilized, pH to 7.3 and filtered again. A total of 500 mL of chelex RPMI was produced. $MgCl_2$ and $CaCl_2$ were added to Chelex-RPMI medium at various concentrations depending on the experiments.

2.2 Methods

2.2.1 Maintenance of Jurkat cell line

Jurkat cells are kept in a suspension culture using RPMI-1640 media which was supplemented with 10 % heat-inactivated fetal bovine serum. The suspended Jurkat cells in RPMI-1640 media were kept in a cell culture incubator at 37°C and 5% CO_2 .

2.2.2 Patch clamp electrophysiology

There are several different types of voltage clamp methods used depending on the type of data to be obtained (Figure 6). Most of these voltage clamp methods begin with the cell attached configuration. This configuration begins with the lowering of the recording pipette to allow the tip to make contact with the cell membrane. A small

negative pressure (i.e. suction) is applied to the recording pipette to form a gigaseal between the glass pipette and the membrane of the cell. This will prevent any ion movement between the recording pipette in the bath and the membrane of the cell. Therefore, any type of ion movement has to occur through the ion channels in the membrane when the voltage changes. This method allows current through the ion channels, within the recording pipette, to be measured.

After the formation of the cell-attached configuration, the whole-cell patch configuration can be created. Applying negative pressure or a short high voltage pulse to the recording pipette can cause the contacting cell membrane patch to rupture. The internal pipette solution will be in contact with the intracellular solutions which will diffuse. Any type of substances can enter the cell and its effect can be measured. The recording electrode in the pipette will record all the ion channels that are present in the cell membrane (Alansary, Kilch, Holzmann, Peinelt, Hoth, & Lis, 2014a; Alansary, Kilch, Holzmann, Peinelt, Hoth, & Lis, 2014b; Kornreich, 2007; Lippiat, 2008; Wickenden, 2014).

The perforated-patch configuration also begins with the cell-attached configuration. The internal solution of the recording pipette contains an ionophore, such as amphotericin B or nystatin, to form ion-permeable pores in the cell membrane while keeping the membrane intact. Small charged monovalent ions are able to pass through these pores. Since there is a flow of charge, these ions carry a current. This allows the study of the activity of all the ion channels in the cell membrane without damaging the

membrane and losing intracellular components, such as Ca^{2+} , Mg^{2+} and ATP (Alansary, Kilch, Holzmann, Peinelt, Hoth, & Lis, 2014a; Alansary, Kilch, Holzmann, Peinelt, Hoth, & Lis, 2014b; Kornreich, 2007; Lippiat, 2008; Wickenden, 2014).

The glass pipettes used were made by Harvard Apparatus PG1207-10 and split in half using a Sutter P-1000 micropipette puller. Each pipette was fire polished to 3 – 5 mOhm resistances using a Narishige MF-830 microforge. The pH of the solutions was maintained at ~7.3 pH measured with a Mettler Toledo SevenCompact pH meter S220.

TRPM7 channel currents were recorded using a HEKA EPC 10 amplifier and HEKA PatchMaster software. The PatchMaster software would apply voltage ramps from -100 to +85 mV every 2.5 seconds during recordings. Since Jurkat cells are free floating, the Jurkat cells were placed on a glass chamber plate and allowed to settle on the bottom for around 10 minutes. The external and internal solutions were chosen in order to isolate currents from TRPM7 channel A standardized external solution contained 140 mM Na-Aspartate, 10 mM HEPES-Na, 0.5 mM D-(+)- Glucose, 2 mM CaCl_2 , 4.5 mM KCl, 3 mM CsCl, pH 7.3, 300 mOsm. External cesium reduces contamination from the inward rectifier potassium channels. Aspartate and glutamate were used in both external and internal solution to reduce the conductance of chloride channels. The internal solution would vary depending on the experiment and type of cell configuration. The internal solution had a pH of 7.3 and 290 mOsm. MgCl_2 was supplemented to the solutions to obtain a certain amount of free Mg^{2+} concentration. The amount of free Mg^{2+}

concentration was estimated using MaxChelator software, located at
<http://web.stanford.edu/~cpatton/maxc.html>

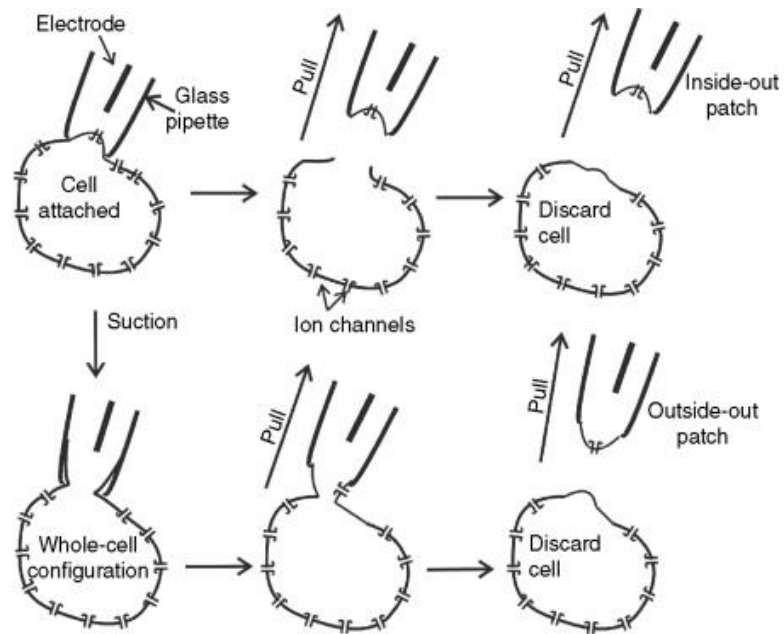


Figure 6: Patch clamp configurations.

A fire polished glass pipette makes contact with the cell membrane and a small negative pressure is applied to achieve a gigaohm seal between the pipette and cell membrane, forming the cell-attached configuration. Whole-cell configuration can be formed from cell-attached by applying a negative pressure or brief high voltage pulses, the contacting cell membrane patch will rupture. The pipette solution will then mix with intracellular solutions. In the perforated-patch configuration an antibiotic such as amphotericin B that can form ion channels in the plasma membrane without rupturing it, is included in the pipette solution. Only monovalent ions are small enough to pass through these pores. Perforated-patch configuration allows the recoding and measurement of ion channels without damaging the membrane and losing intracellular components or altering intracellular Mg^{2+} (Reproduced from Petkoy, 2009 with permission).

2.2.3 Intracellular Ca²⁺ imaging

The Ca²⁺ imaging experiments used extracellular solutions shown in Table 2. The primary solution is the 2 Ca²⁺ basal solution which contains: 2 mM CaCl₂, 140 mM NaCl, 4 mM KCl, 10 mM D-(+)-Glucose and 10 mM HEPES-Na, pH 7.3 and osmolarity 300. The second solution was Ca²⁺-free solution containing: 1 mM EGTA, 10 mM HEPES-Na, 10 mM D-(+)-Glucose, 4 mM KCl, 140 mM NaCl, pH 7.3 and osmolarity 300. 20 μM of CPA and 20 μM of ionomycin were used. The cells were loaded with 4 μM Fura-2 AM ratiometric calcium dye indicator in the 2 Ca²⁺ basal recording solution supplemented with 20% Pluronic in DMSO.

The 35 mm glass-bottom chambers were cleaned using 70% ethanol along with gently scraping the glass with a pipette tip, rinsed with ddH₂O and wiped clean with a kimwipe sprayed with 70% ethanol. Since the Kimwipe can leave fibers, the glass-bottom chambers were rinsed off with ddH₂O and any remaining liquid aspirated off. Next, the glass-bottom chambers were double coated using a high molecular weight poly-d-lysine. The glass is covered with poly-D-lysine solution and allowed to sit for 15-20 minutes. Poly-d-lysine is aspirated off and the glass portion is recovered for an additional 15 minutes. After 15 minutes, the poly-D-lysine is aspirated off until it is dry. About 250-300 μL of cells were used to cover the glass portion. The cells were allowed to adhere to the chambers for 20 minutes at room temperature.

Once the cells adhered to the chambers, they were loaded with the dye solution in a dark room. The culture media was removed and the dye-containing solution is

immediately added. About 250-300 μL of dye solution is used to cover the chambers. Then the chambers are placed in a dark incubator at 37°C for ~45 minutes. This provides enough time for Fura 2-AM to diffuse into the cell. After 45 minutes, the dye solution is removed and the 2 Ca^{2+} basal solution is added. The cells will remain in the 2 Ca^{2+} solution for about 20 minutes to allow cytosolic esterases to cleave the -COOH groups of Fura 2-AM, thus allowing Fura 2 to regain its charge to bind calcium and be unable to diffuse out of the cell.

To perform Ca^{2+} imaging, an Olympus CKX41 inverted microscope was connected to a Dell Optiplex 745C computer with InCytIM 2 imaging program (Intracellular Imaging, Cincinnati, OH) installed. 175 W Xenon arc lamp provided the UV light source and the filters in Lambda 10-B SmartShutter allowed selections of the wavelength. After the cleavage step, the cells are positioned on the stage of the microscope. The perfusion rate was ~20 ml per minute using the corresponding solutions for the different experiments. Throughout the designated time frame, the cells were exposed to 340 nm and 380 nm wavelengths with a switch rate of 40 milliseconds. InCytIM 2 imaging program was recording the emitted light at 510 nm.

Ca^{2+} imaging was able to measure from up to 99 cells per experiment. Each cell would produce its own data and wavelength trace. Selecting which cell to use was based on a few behaviors: (i) the initial 2 Ca^{2+} perfusion maintain a relatively stable base line over time; (ii) the 340 nm and 380 nm wavelength traces moved in opposite directions from each other during the course of the recording; (iii) when CPA was perfused, the cell

was able to respond to CPA; (iv) the cell was not lost during the recording. v) ionomycin elicited a robust Ca^{2+} increase.

Table 2: Ca²⁺ Imaging solutions

Salts & Solutions	Concentration in "2 Ca ²⁺ solution"	Concentration in "Ca ²⁺ free solution"
CaCl ₂	2 mM	
NaCl	140 mM	140 mM
KCl	4 mM	4 mM
D-(+)-Glucose	10 mM	10 m
HEPES-Na	10 mM	10 mM
EGTA		1 mM
CPA		20 μM
Ionomycin		20 μM

2.2.4 Vi-Cell viability analyzer

A Beckman Vi-Cell cell viability analyzer is able to perform single cell measurements to give the size and number of the cells in the sample, provide the percent of viable cells and take real-time cell images (Gibson, Beesetty, Sulentic, & Kozak, 2016). The Vi-cell uses trypan blue dye to determine cell viability. Trypan blue is able to be taken up by dead cells since the membrane of dead cells becomes permeable. The non-viable cells are stained with the trypan blue becoming darker than the viable cells. The analyzer is able to do 15 samples within an hour. After collecting the data, the software will export the data in a spreadsheet and save the pictures of each measurement. If there is debris in the sample, the analyzer may treat the debris as viable cells. There are some drawbacks of using the Vi-Cell viability analyzer. When the sample is mixed with trypan blue and loaded into the analyzer, air bubbles may form during this process. The air bubbles will cause distortion when the analyzer takes pictures of the cell which will have an effect on the measurement of the cell diameters. Samples with air bubbles were omitted. In addition, the software analyzer forms circles around the cells during measurement. Non-spherical cells will have issues due to the method of measurement. The resulting data obtain may be skewed towards the long axis.

2.2.5 Osmolality of solutions

The osmolality of the solutions was measured using a Precision System Inc. 5004 MICRO-OSMETTE Automatic High Sensitivity 50 μ L Osmometer. Three different disposable sample tubes was filled with 50 μ L solution, then each was measured in rapid

succession to determine the average osmolarity of the solution. If the osmolarity was too low, the appropriate amount of D-mannitol was added to increase the osmolarity. An osmolality of 300 was used for the external solutions. The internal solution osmolality was around 285 to 300.

2.2.6 Data Analysis

OriginLab 8 software was used to analysis the data and create the graphs. The statistical analysis was determined using ANOVA and Student's t-test. The data was considered to be significant difference if $p < 0.05$. The standard error of the mean is shown as the error bars in the graphs.

III. Results

3.1 Endogenous TRPM7 channels of Jurkat T cells can be used as a bioassay of external Mg^{2+} concentration.

TRPM7 is inhibited by intracellular concentrations of free Mg^{2+} ranging from 0.3 to 1 mM and the cell has around 0.5 to 1 mM of free cytosolic Mg^{2+} . Under physiological conditions, TRPM7 channels are rendered inactive in intact Jurkat cells. Since depletion of magnesium should result in the activation of TRPM7 channel, Jurkat cells were grown in low magnesium conditions to determine if the TRPM7 has the ability to become activate and produce a current. Chelex-100 was used to remove divalent metal cations such as calcium and magnesium from RPMI-1640. Then the cation depleted RPMI was supplemented with a 6 μ M $MgCl_2$ and 1.4 mM $MgCl_2$ to simulate magnesium deficiency conditions, while the initial RPMI-1640 Ca^{2+} concentration of 0.4 mM remain constant. Over time, the internal magnesium concentrations of the Jurkat cells is expected to be depleted. Jurkat cells were allowed to grow in the chelex RPMI with different magnesium concentrations from 24 hours to 48 hours or longer.

Vi-Cell viability analyzer was used to confirm the viability of the cells and average diameters of the cells as well (Figure 13). Patch clamp was performed to obtain the break-in current before the pipette solution diffuses into the cell and the maximum current at 83.47 mV. Dividing the break in current over the maximum current was used to obtain the preactivation index, which allows the comparison of the degree of activation in intact cells. The preactivation index of the Jurkat cells grown in 6 μ M $MgCl_2$ and 1.4 mM

MgCl₂ was different from each other. The Jurkat cells grown in lower Mg²⁺ concentration had a larger preactivation index (Figure 7).

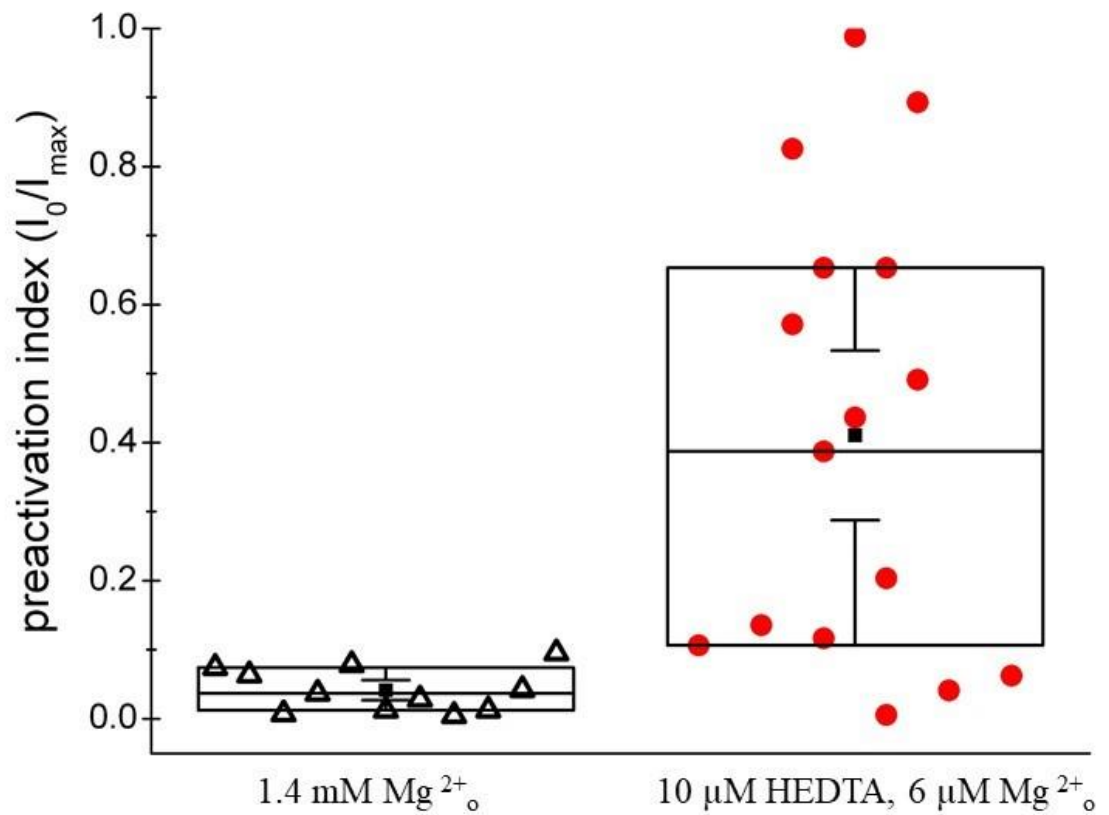


Figure 7: TRPM7 channel activity during Mg⁺ loading and depletion.

Jurkat cells cultured for 24 to 48 hours in Chelex RPMI supplemented with 6 μM MgCl₂, 10 μM HEDTA or 1.4 mM MgCl₂ and at constant 0.42 mM CaCl₂. Box graph was plotted using TRPM7 preactivation index. Error bars represented as mean ± SEM (p<0.05).

The Jurkat cells were cultured in different concentrations of Mg^{2+} ranging from 400 nM to 1.4 mM for 24 – 48 hours (Figure 8). Over time, a decrease in external Mg^{2+} concentration will be reflected in the intracellular Mg^{2+} concentration. Without Mg^{2+} inhibition, TRPM7 channel will become activated and the current value should show a relation to the amount of external Mg^{2+} . The preactivation index shows that the Jurkat cells grown in lower Mg^{2+} concentrations were associated with a larger preactivation index and the preactivation index value decreased as the external Mg^{2+} concentration was increased (Figure 8A). The dose-response relation in OriginLab software was used to fit the data to obtain the IC_{50} and Hill coefficients. The IC_{50} was 54 μ M (Figure 8B).

Splenic T cells were obtained from a WT mouse and KD mutant mouse. The T cells were grown in chelex RPMI supplemented with an increasing Mg^{2+} concentration and a constant $CaCl^{2+}$ concentration at 0.424 mM. Then the T cells were stimulated with PMA/ionomycin. The proliferation rates of the T cells were measured using MTS colorimetric assay at 24 hours and 48 hours after activation of the T cells. Figure 9A shows the proliferation rate of the KD T cells was reduced compared to the WT T cells proliferation after 24 hours after activation. When the T cells were allowed to proliferate for 48 hours (Figure 9B), the proliferation increased for both the WT and KD T cells. However, the KD T cells proliferation rate was significantly decreased compared to the WT T cells. At 48 hours, the IC_{50} value of the KD T cells were 52 μ M and the Hill coefficient was 1.46 (from Beesetty et al, 2018).

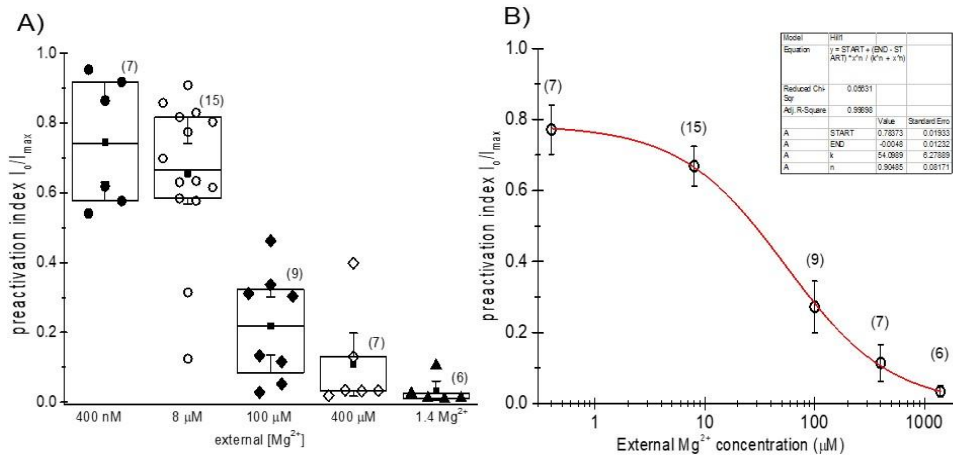


Figure 8: Extracellular Mg^{2+} dose-response relation.

A dose response relation was plotted using Jurkat cells grown in 5 different extracellular Mg^{2+} concentrations, ranging from 400 nM to 1.4 mM, for 24 - 48 hours. Patch-clamp electrophysiology was performed to obtain the preactivation index from the each Jurkat cell. 8A is a box graph plotted with the preactivation index against external $[\text{Mg}^{2+}]$. Error bars represent mean \pm SEM. 8B is dose-response relation of external $[\text{Mg}^{2+}]$. Error bars are represented as mean \pm SEM. Numbers of cells are in parentheses.

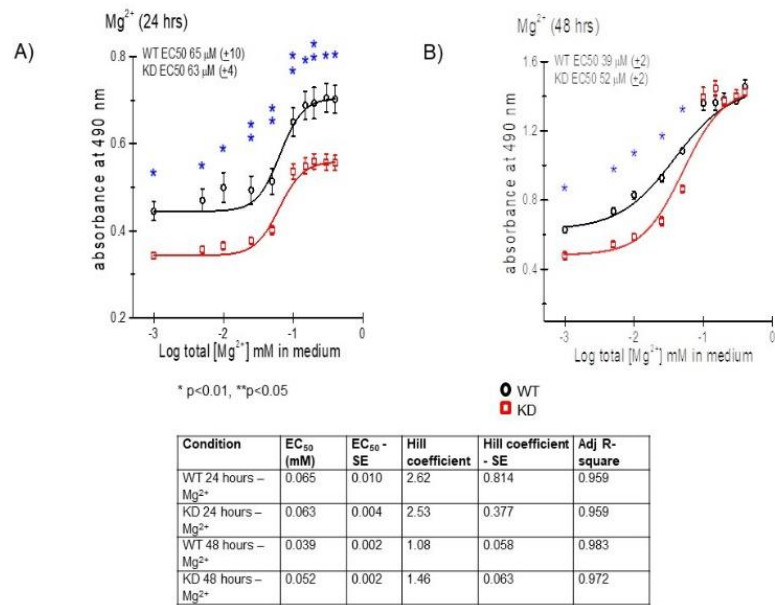


Figure 9: Proliferation of WT and kinase-dead (KD) mouse T cells in increasing external Mg²⁺ concentrations

Proliferation rate of activated KD T cells and WT T cells was compared. Both T cell groups were grown in an increasing external Mg²⁺ concentrations from 0.001 – 0.4 mM MgCl₂ while the Ca²⁺ concentration remained constant at 0.424 mM. Proliferation measurements were taken at 24 hours in Figure 9A and 48 hours in Figure 9B. Error bars are represented as mean ± SEM (p<0.01, p<0.05). (After Beesetty et al, 2018)

The Mg^{2+} depletion and loading in the Jurkat T cells is proposed to be governed by Na^+/Mg^{2+} antiporter. Jurkat cells were cultured in chelex RPMI supplemented with 1.4 mM $MgCl_2$, 10 μ M HEDTA and 0.42 mM $CaCl_2$ for 24 hours. Then these Jurkat cells were switched to two different RPMI conditions for 24 hours – 48 hours. In the first condition, the Jurkat cells was treated with 10 μ M HEDTA, 10 μ M $MgCl_2$ and 300 μ M amiloride. In the second condition, a control group of Jurkat cells was grown without the 300 μ M amiloride treatment. Patch clamp experiments were performed on those Jurkat cells at 24 hours and 48 hours to obtain the initial break-in current and maximum current. After 24 hours, there was a significant difference between the amiloride treated Jurkat cells and the Jurkat cells without amiloride treatment. The amiloride treated Jurkat cells had a smaller break-in current shown in Figure 10A. In Figure 10B after 48 hours, the break-in current was reduced in Jurkat cells treated with and without amiloride. However, the amiloride treated cells still retain the smaller break-in current when compared to the Jurkat cells without amiloride treatment. The maximum current was similar to the break-in current, in which the amiloride treated Jurkat cells also had a lower maximum current when compared to the Jurkat cells without amiloride treatment after 24 hours in Figure 10C and after 48 hours in Figure 10D. The preactivation index indicates there was a significant difference between the Jurkat cells with the amiloride treatment and without amiloride, shown in Figure 11A and Figure 11B.

The reversed experiment was performed using the Jurkat cells cultured in low Mg^{2+} . The low Mg^{2+} Jurkat cells were treated with 1.4 mM $MgCl_2$, 10 μ M HEDTA and

0.42 CaCl₂ RPMI with and without 300 μM amiloride. After 24 hours, the preactivation index was obtained. Figure 11C reveals there was no significant difference between the two conditions. The preactivation index of the Jurkat cells without amiloride was reduced to a similar value of the amiloride treatment.

Jurkat cells were cultured in chelex RPMI with 10 μM MgCl₂, 10 μM HEDTA and 0.42 CaCl₂ for a 48 hours. Perforated patch configuration was performed using an internal pipette solution containing 7 mM MgCl₂. The internal Mg²⁺ concentration was depleted and a large current was observed. A current-voltage relation and time course was plotted in Figure 12. Figure 12B shows the time course in the same cell as Figure 12A. The Jurkat cell membrane was ruptured in to confirm the perforated patch configuration. Upon the membrane rupture, the pipette Mg²⁺ will diffuse into the cell and inhibit the TRPM7 channel. The inhibition of TRPM7 is shown as the drop in the current.

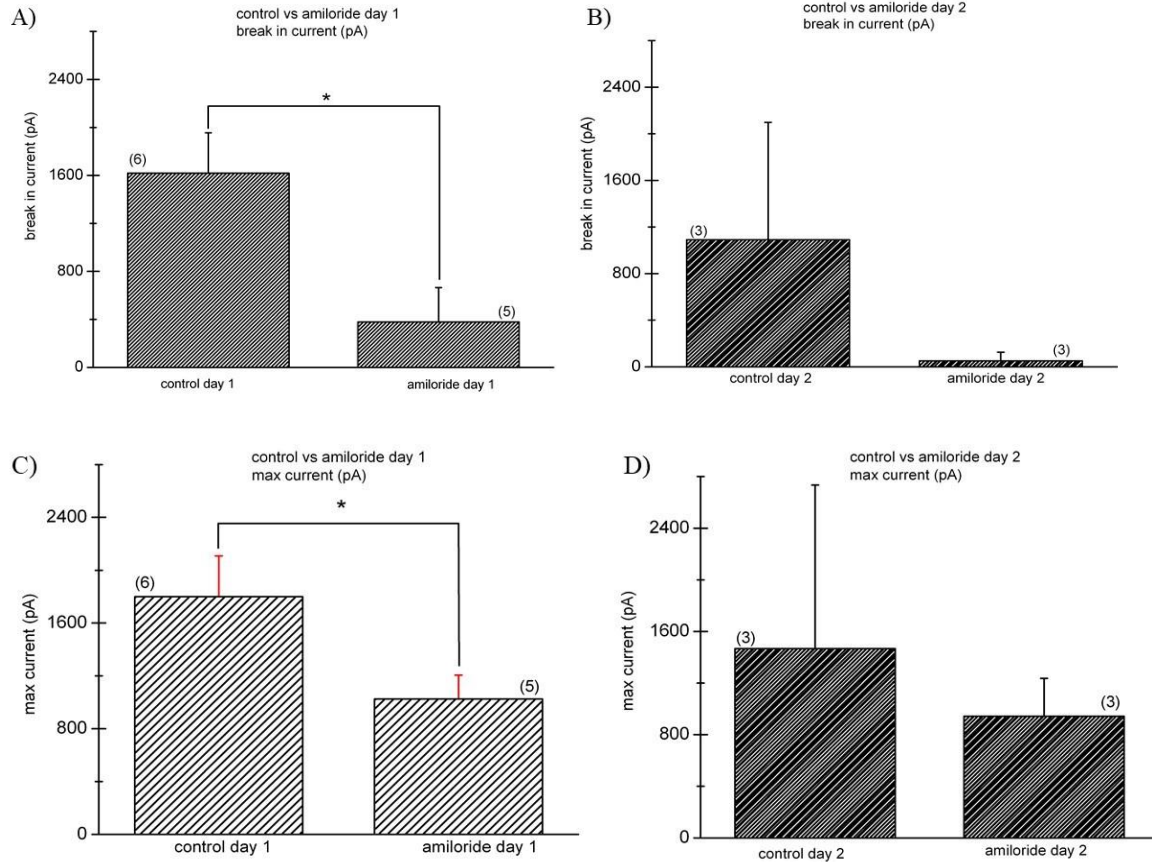


Figure 10: Amiloride sensitivity of TRPM7 currents

The break-in and maximum current was plotted in amiloride treated and untreated Jurkat cells. 10A shows that there was a significant difference between the break-in currents of control and amiloride grown cells after 24 hours. At 48 hours, there was a reduction in the break-in currents for both conditions in 10B. The maximum current was reduced by amiloride treatment for 24 hours in 10C and 48 hours in 10D. Error bars represent mean \pm SEM ($p < 0.05$).

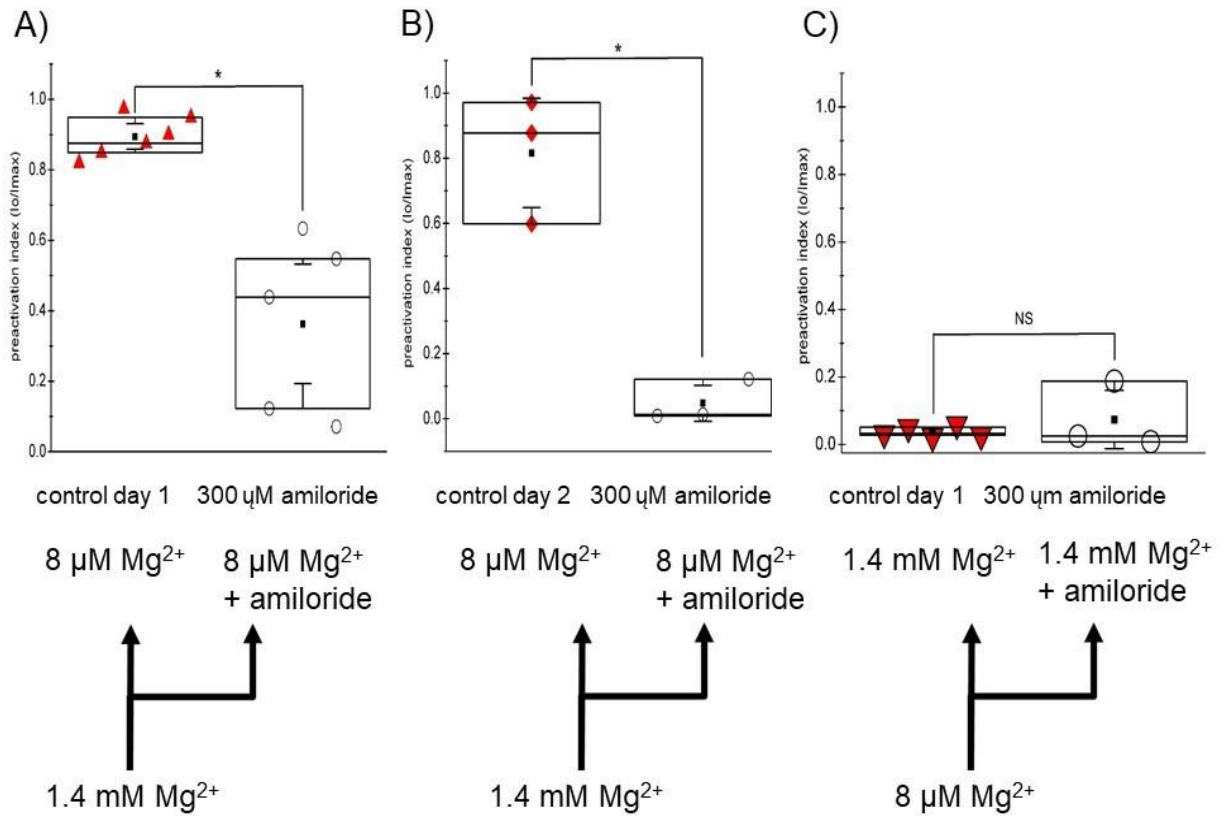


Figure 11: Amiloride sensitivity of Mg²⁺ efflux and influx in Jurkat T cells.

There was a significant difference between cells treated with or without 300 μM amiloride. The preactivation index of the 300 μM amiloride treated Jurkat cells was lower compared to the control cells in 11A. 11B was measured after 48 hours. The amiloride treated Jurkat cells had a smaller preactivation index compared to the non-treated Jurkat cells. In 11C cells were loaded with Mg²⁺ after being depleted in 8 μM lead to reduced preactivation index which was insensitive to amiloride. Error bars are mean ± SEM (p<0.05).

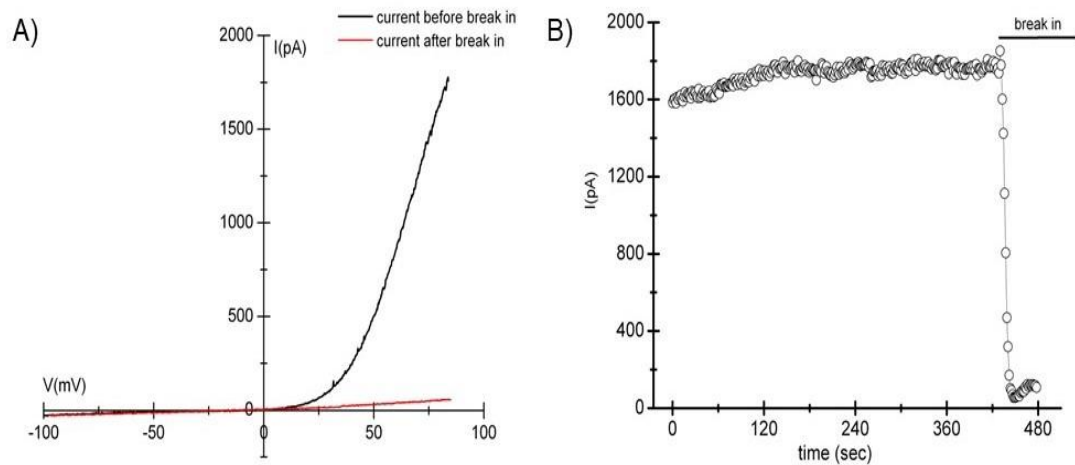


Figure 12: I-V and time dependence of TRPM7 current in Mg^{2+} -depleted Jurkat T cells.

12A shows current-voltage relation of TRPM7 current from Jurkat cells grown in chelex RPMI with $10 \mu M$ $MgCl_2$, $10 \mu M$ HEDTA and $0.42 CaCl_2$ for 48 hours. Internal Mg^{2+} was depleted and a large current was observed in perforated patch (black trace). The red trace is the current measured after the cell membrane was ruptured and whole-cell patch clamp configuration formed. 12B shows the time course of the TRPM7 in the same cell as 12A. The rupture of the membrane occurred at the break-in mark.

3.2 MagT1 knock-out (KO) Jurkat T cells have lower cytoplasmic concentrations of Mg^{2+} as determined by TRPM7 channel activity.

Due to the nonfunctional MagT1 of MagT1 KO Jurkat cells, the influx of Mg^{2+} and free cytosolic Mg^{2+} concentration should be reduced when compared to the WT92 Jurkat cells. The Mg^{2+} concentration could be reduced enough to allow the activation of TRPM7. The WT92 Jurkat cell and MagT1 KO Jurkat cell lines are used. Both cell lines were culture in RPMI with 30 μ M $MgCl_2$ and 1 mM $MgCl_2$ for a few days to determine the viability and proliferations of the cells. After 96 hours, a Vi-Cell viability analyzer shows both cell lines were viable and able to proliferate and in both RPMI conditions without any issues (Figure 13).

The K^+ current has an influence to promote Ca^{2+} influx and since MagT1 mechanism remains unknown, the influence of MagT1 on K^+ channels was investigated. The Jurkat cells were cultured in RPMI supplemented with a low concentration of Mg^{2+} to deplete the cells. Perforated patch clamp was performed using a K^+ based internal solution containing 55 mM KCl, 70 mM K_2SO_4 , 7 mM $MgCl_2$, 1 mM $CaCl_2$ and 10 mM HEPES. Two different K^+ based external solutions were used; a low K^+ external solution of 140 mM Na-aspartate, 2 mM $CaCl_2$, 10 mM HEPES-Na, 4.5 KCl and a high K^+ external solution with 140 mM K-aspartate, 2 mM $CaCl_2$, 10 mM HEPES-Na, 4.5 NaCl. During the patch clamp recording, the K^+ based external solution was perfused at a late time frame. The I-V relation was plotted in Figure 14.

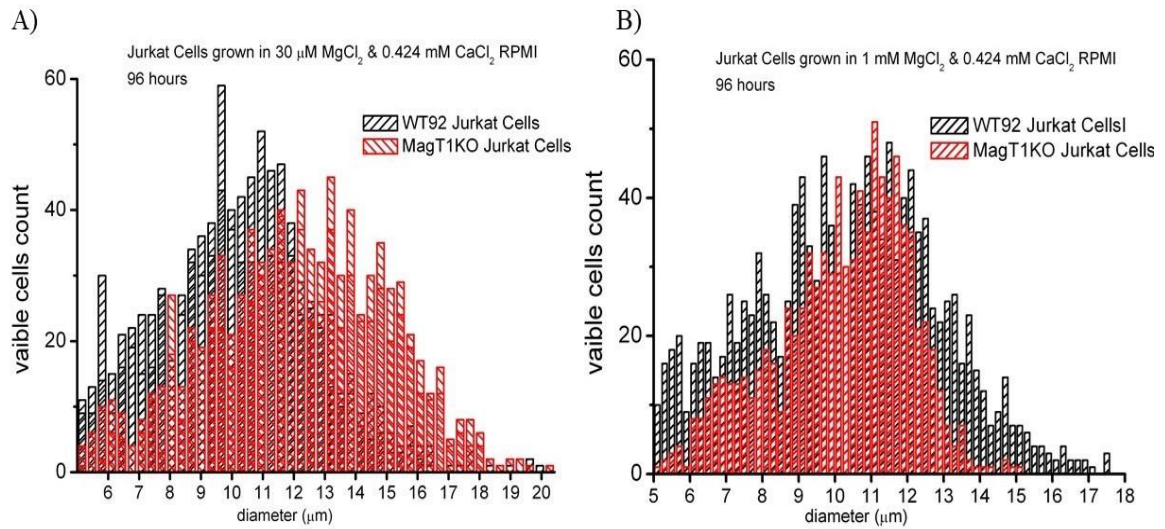


Figure 13: Viability and diameters of Jurkat cells grown in chelex RPMI supplemented with Mg^{2+} for 96 hours.

Histogram of the Jurkat cell diameters cultured in Mg^{2+} supplemented chelex RPMI for 96 hours. Vi-Cell viability analyzer was used to measure cell viability and diameters of Jurkat cells.

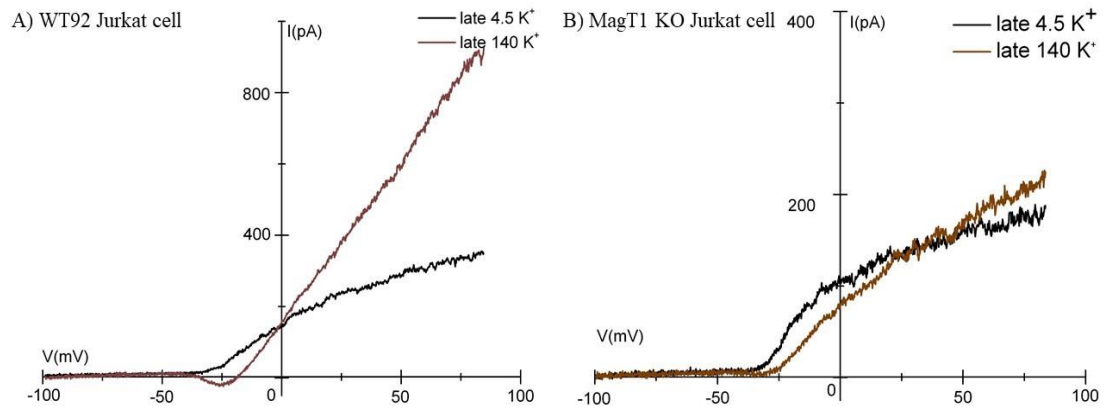


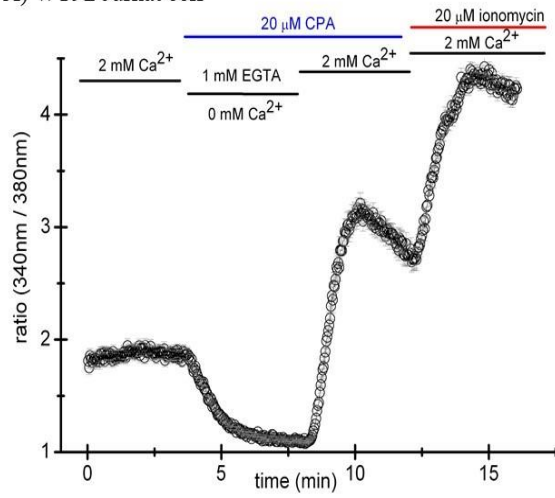
Figure 14: I-V relations using K^+ -based internal in WT and MagT1 KO Jurkat cells

I-V relation of WT and MagT1 KO Jurkat cells. The black trace indicates the perfusion of low K^+ external solution late in the patch clamp measurement. The brown trace indicates the perfusion of the high K^+ external solution late in the patch clamp recording.

Since Ca^{2+} entry and CRAC are both required for T-cell proliferation, Ca^{2+} imaging was performed to look into the effects MagT1 might have on Ca^{2+} . Ca^{2+} imaging was performed. Fura-2 AM calcium indicator dye was loaded into the T Jurkat cells and MagT1 KO Jurkat cells to measure the intracellular Ca^{2+} levels (Figure 15). A baseline intracellular Ca^{2+} level was recorded with external 2 mM Ca^{2+} solution. During the recording, different solutions were perfused at set time intervals. The next solution to be perfused contains 20 μM CPA, 1 mM EGTA and 0 mM Ca^{2+} . CPA inhibits the SERCA pump, resulting in the depletion of ER Ca^{2+} stores and activation of SOCE. The intracellular Ca^{2+} will decrease below the baseline intracellular Ca^{2+} level. Since the ER Ca^{2+} stores are depleted, CRAC channels will form. Then a solution containing 20 μM CPA, 1 mM EGTA and 2 mM Ca^{2+} is perfused. There is an influx of Ca^{2+} , which is the sudden spike in the ratios in Figure 15. And the last solution of 20 μM ionomycin and 2 mM Ca^{2+} was perfused to obtain a positive control. The baseline intracellular Ca^{2+} levels were similar in both WT Jurkat cells and MagT1 KO Jurkat cells. Upon depletion of ER Ca^{2+} stores and activation of CRAC, the Ca^{2+} influx was similar in the both the MagT1 KO Jurkat cells (Figure 15B) and the WT92 Jurkat cells (Figure 15A).

The CRAC current was measured using patch clamp. The I-V relations of the CRAC current in WT Jurkat cells (Figure 16A) and MagT1 KO Jurkat cells (Figure 16B) was obtained using a Ca^{2+} based solution. When the I-V relations was compared, there was no significant difference between the cell lines (Figure 17).

A) WT92 Jurkat cell



B) MagT1KO Jurkat cell

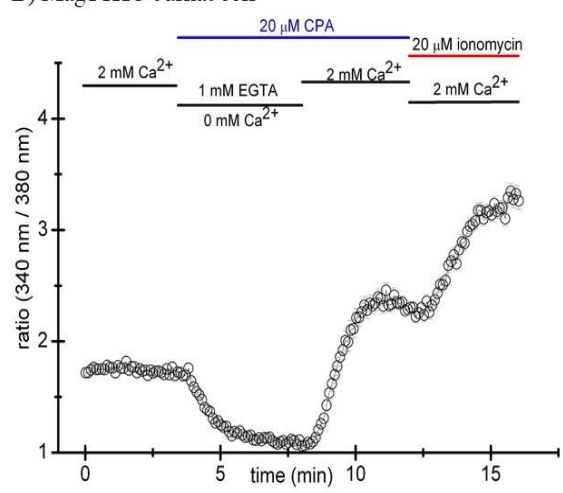


Figure 15: Ca²⁺ imaging in WT and MagT1 KO Jurkat cells.

Fura-2 AM calcium indicator dye was loaded into Jurkat cells to perform intracellular Ca²⁺ imaging and measure SOCE. Error bars are represented as mean ± SEM.

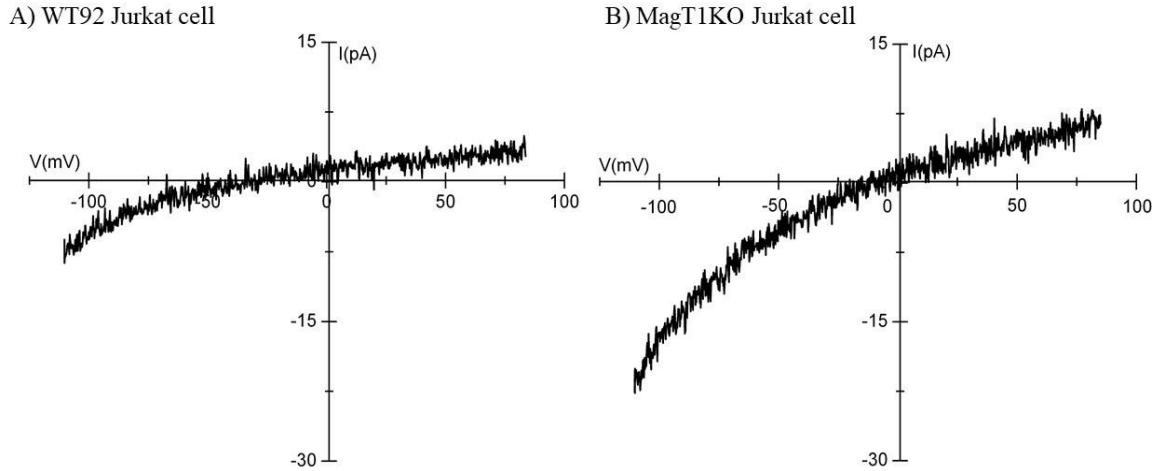


Figure 16: Store-operated CRAC currents in WT and MagT1 KO Jurkat cells.

I-V relations of CRAC currents in WT92 Jurkat cell in 16A and MagT1 KO Jurkat cell in 16B.

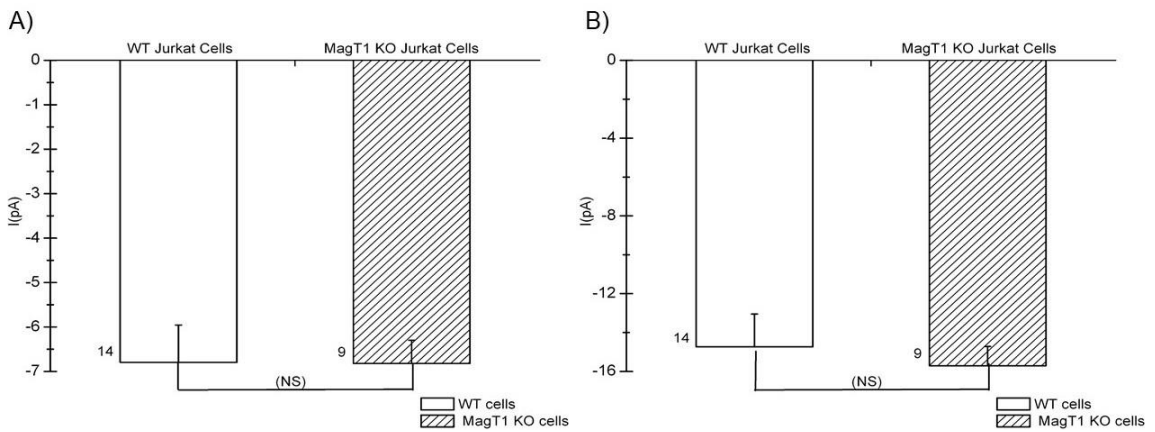


Figure 17: Bar graphs of CRAC amplitudes in WT and MagT1 KO Jurkat cells.

17A is bar graph comparing the initial break-in currents. The maximum current of the CRAC current on compared in 17B. There were no significant differences between the initial break in currents or maximum currents in WT vs. MagtT1 KO cells. Error bars are mean \pm SEM ($p < 0.05$).

The MagT1 KO Jurkat cell is expected to have a lower concentration of intracellular Mg^{2+} and the TRPM7 should be expected to produce a larger current than the WT92 Jurkat cells. The outwardly rectifying I-V relation of TRPM7 current was measured using whole cell patch clamp in Figure 18. The internal solution of the pipette contained 30 μM of free Mg^{2+} , which would diffuse into the cell and was sufficient enough to allow activation of TRPM7 channels. When the I-V relation was compared, there was a significant difference between the WT92 Jurkat Cells (Figure 18A) MagT1 KO Jurkat cells (Figure 18B). The concentration of free Mg^{2+} in the internal solution was increased to 400 μM . The I-V relation of TRPM7 current in the WT92 Jurkat cells (Figure 18C) and MagT1 KO Jurkat cell (Figure 18D) was plotted.

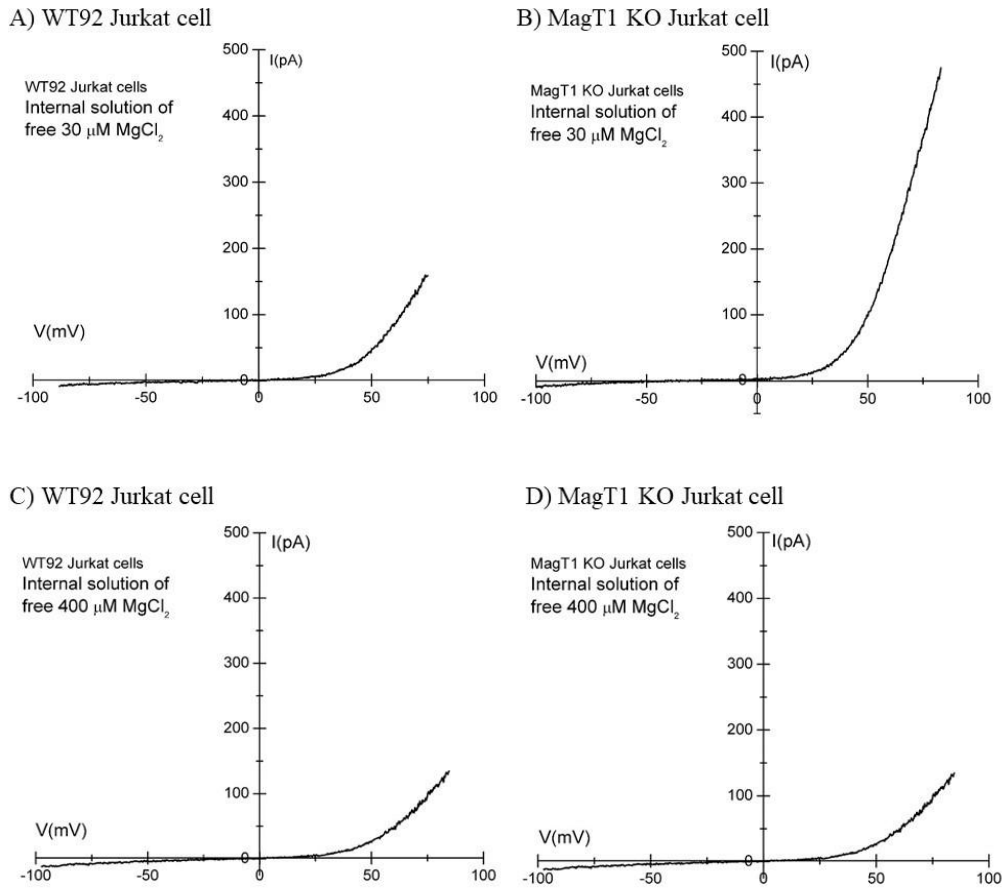


Figure 18: TRPM7 I-V relations of WT92 and MagT1 KO Jurkat cells.

I-V relations of WT92 and MagT1 KO Jurkat cells using a pipette internal solution of free 30 μM MgCl_2 and free 400 μM MgCl_2 . The internal solution of the pipette contains free 30 μM MgCl_2 in 18A and 18B. The MagT1 KO Jurkat cell in 18B produced a larger TRPM7 current than the WT92 Jurkat cell in 18A. When the internal solution of the pipette contained 400 μM MgCl_2 in 18C and 18D, the TRPM7 current of MagT1 KO in 18D was reduced. The WT92 TRPM7 current in 18C was similar to 18A.

IV. Discussion

Mg^{2+} is the one of the most abundant cations and has important roles within the body, ranging from functioning as an enzyme cofactor to development. However, Mg^{2+} physiology and homeostasis remain relatively unknown for such an important metal cation. TRPM7 is believed to be a key component of cellular Mg^{2+} homeostasis. MagT1 is a highly selective Mg^{2+} transporter but its precise physiological function remains unknown as well. The activation of T cell receptor (TCR) was reported to result in activation of MagT1 by an unknown pathway, causing rapid Mg^{2+} influx. Without proper MagT1 function, Mg^{2+} influx may become impaired and the cell development and proliferation will be negatively affected.

Jurkat cells were cultured in low Mg^{2+} RPMI conditions to determine if endogenous TRPM7 has the ability to act as a bioassay for external Mg^{2+} . Experiments were performed using Jurkat cells grown in different concentrations of Mg^{2+} , ranging from 400 nM to 1.4 mM for 24 – 48 hours (Figure 7 and 8A). When the extracellular Mg^{2+} concentration was reduced for 1-2 days, the intracellular Mg^{2+} was depleted. Without intracellular Mg^{2+} inhibition, the TRPM7 channels would become pre activated and produce a current. The preactivation of the current showed a relation to the amount of external Mg^{2+} . As the extracellular Mg^{2+} concentration was increased, the Jurkat cells had less preactivation of TRPM7 channels when compared to the Jurkat cells cultured in lower Mg^{2+} concentration (Figure 8A). Conversely, incubation in elevated Mg^{2+} is sufficient to eliminate TRPM7 channel activity at break-in, corresponding to the situation

in an intact cell. Using this approach, extracellular Mg^{2+} dose-response relation can be constructed for TRPM7 channels (Figure 8B). The dose-response relation in OriginLab software was used to fit the data to obtain the IC_{50} and Hill coefficients. The IC_{50} was 54 μM which shows that half of the channels in the membrane are closed at that Mg^{2+} concentration (Figure 8B).

The IC_{50} of the Mg^{2+} dose response in Figure 8B was similar to the IC_{50} of the proliferation rate of murine T-cells in Figure 9. The resting TRPM7 KD mutant T cells diameters were slightly larger than WT T cells (Beesetty et al, 2018). Upon stimulation of the resting TRPM7 KD mutant T-cells, the proliferation and cell diameters grew less compared to the WT T-cells. A similar effect has been seen in the low magnesium grown Jurkat cells compared to the high magnesium grown Jurkat cells. There is a possibility the changes in blastogenesis and proliferation could occur through the same mechanism. While the resting TRPM7 mutant T-cells involved a kinase dead mutation in Figure 9, a dose-response was performed to investigate the influences of ions. The internal magnesium concentrations could be affected through an unknown mechanism that has a role in proliferation. The data suggest T-cell proliferation may be dependent on the degree of TRPM7 current activation. These changes could occur due to the low magnesium environment.

Overall the free cytoplasmic Mg^{2+} concentration is similar to extracellular Mg^{2+} concentration (Chokshi, Matsushita, & Kozak, 2012a). The membrane potential of Jurkat T cells is around -55 to -65 mV (Verheugen, Vijverberg, Oortgiesen, & Cahalan, 1995).

The calculations for the Nernst potential indicate that the concentration of intracellular Mg^{2+} must be much higher since there is an inward electrogenic driving force. However, the data in Figure 11 suggest the external and internal Mg^{2+} concentration are essentially the same. Mg^{2+} efflux in Jurkat cells is amiloride sensitive, while the Mg^{2+} influx is not amiloride sensitive. The amiloride sensitivity effect is most likely due to Na^+/Mg^{2+} antiporter becoming inhibited by amiloride (Romani, 2011). The membrane potential does not have an influence on the accumulation of Mg^{2+} .

The use of TRPM7 for estimating cellular Mg^{2+} has several advantages over fluorescent Mg^{2+} dyes, one of which is a much broader dynamic range. Overall, we find that endogenous TRPM7 channels of Jurkat T cells can be used as a bioassay of external Mg^{2+} concentrations.

MagT1 knocked out Jurkat T cells will prevent Mg^{2+} influx and appear to have lower internal cytoplasmic concentrations of Mg^{2+} . The WT92 Jurkat cells and MagT1 Jurkat cells were cultured in chelex RPMI supplemented with 30 μ M $MgCl_2$ and 1 mM $MgCl_2$ at 96 hours. Then Vi-Cell viability analyzer was used to determine the viability and proliferation of the cells. Both cell lines were able to survive and proliferate in different Mg^{2+} conditions (Figure 13). The influences of MagT1 on K^+ channels and CRAC (ORAI/STIM) channels were looked into by performing patch clamp and Ca^{2+} imaging. The K^+ channels were expressed and functioning in the MagT1 KO cells (Figure 14). MagT1 does not appear to have any influences on K^+ currents and the membrane potential of the MagT1 KO Jurkat cells is not expected to be any different

from the WT92 Jurkat cells. There was no significant difference in the Ca^{2+} imaging (Figure 15) and I-V relation of CRAC (Figure 16). Thus, impaired Mg^{2+} influx does not appear to affect the K^+ channels and CRAC channels functionality, suggesting MagT1 or Mg^{2+} does not have any role in function of K^+ channels and CRAC channels.

When the cytoplasmic concentration of Mg^{2+} is reduced, TRPM7 channels should become activate and a TRPM7 current would be observed. An internal solution of 30 μM of free Mg^{2+} was used in patch clamp on the WT92 Jurkat cells and MagT1 KO Jurkat cells. The MagT1 KO Jurkat cells show higher pre-activated current, indicating that there is less Mg^{2+}_i and therefore less inhibition of TRPM7 current (Figure 18B). The sensitivity of TRPM7 could have been affected in the MagT1 KO Jurkat cells. In order to check the sensitivity of TRPM7, the concentration of free Mg^{2+} in the internal solution was increased to 400 μM and the I-V relations of both Jurkat cells were obtained. The TRPM7 current in the MagT1 KO Jurkat cell was reduced (Figure 18D), indicating the Mg^{2+} sensitivity of TRPM7 was not affected in the MagT1 KO Jurkat cells. The TRPM7 channel was able to reflect the internal concentration of Mg^{2+} .

In addition, Jurkat cells cultured in low external Mg^{2+} conditions resulted in the depletion of intracellular Mg^{2+} . With the reduction of intracellular Mg^{2+} , TRPM7 currents should produce a large current, as shown in Figure 12A. Jurkat cells cultured in normal Mg^{2+} conditions (Figure 3) were unable to produce a large TRPM7 current.

The nonfunctional MagT1 did not allow Mg^{2+} influx in the MagT1 KO cells, which appears to have an effect by reducing the intracellular concentration of Mg^{2+} . We

showed that the TRPM7 channel became activated, demonstrating that TRPM7 can be used to determine the intracellular Mg^{2+} concentrations.

V. Conclusion.

Endogenous TRPM7 channel activity can be used as a bioassay for cytoplasmic concentration of Mg^{2+} in Jurkat T cells, due to the unique ability of TRPM7 to be inhibited by cytoplasmic free Mg^{2+} . This feature will allow the amount of cytoplasmic Mg^{2+} to be represented as the degree of TRPM7 activation or inhibition. The external Mg^{2+} environment will influence the internal concentrations of Mg^{2+} in Jurkat T cells. Eliminating MagT1 will affect the internal Mg^{2+} concentration, suggesting MagT1 could be an important pathway for Mg^{2+} entry. The reduction of internal Mg^{2+} will result in the activation of TRPM7 channel and higher pre-activated current, while the reduction of cytoplasmic Mg^{2+} does not appear to have an effect on the function of Ca^{2+} and K^+ channels. Internal Mg^{2+} concentrations and the degree of TRPM7 activation could have a role in T cell proliferation. Overall Mg^{2+} physiology function and pathways remain a mystery and TRPM7 can be used as a bioassay for cytoplasmic concentration of Mg^{2+} in Jurkat T cells which will aid in uncovering the physiological roles of intracellular Mg^{2+} .

References

- Abraham, R. T., & Weiss, A. (2004). Jurkat T cells and development of the T-cell receptor signalling paradigm. *Nature Reviews.Immunology*, 4(4), 301-308. doi:10.1038/nri1330 [doi]
- Ahmed, F., & Mohammed, A. (2019). Magnesium: The forgotten electrolyte-A review on hypomagnesemia. *Medical Sciences*, 7(4), 10.3390/medsci7040056. doi:E56 [pii]
- Alansary, D., Kilch, T., Holzmann, C., Peinelt, C., Hoth, M., & Lis, A. (2014a). Measuring endogenous ICRAC and ORAI currents with the patch-clamp technique. *Cold Spring Harbor Protocols*, 2014(6), 630-637. doi:10.1101/pdb.prot073254 [doi]
- Alansary, D., Kilch, T., Holzmann, C., Peinelt, C., Hoth, M., & Lis, A. (2014b). Patch-clamp measurement of ICRAC and ORAI channel activity. *Cold Spring Harbor Protocols*, 2014(6), 602-607. doi:10.1101/pdb.top066795 [doi]
- Bessac, B. F., & Fleig, A. (2007). TRPM7 channel is sensitive to osmotic gradients in human kidney cells. *The Journal of Physiology*, 582(Pt 3), 1073-1086. doi:jphysiol.2007.130534 [pii]
- Beesetty, P., Wiczerzak, K. B., Gibson, J. N., Kaitsuka, T., Luu, C. T., Matsushita, M., & Kozak, J. A. (2018). Inactivation of TRPM7 kinase in mice results in enlarged

spleens, reduced T-cell proliferation and diminished store-operated calcium entry.

Scientific Reports, 8(1), 3023-018-21004-w. doi:10.1038/s41598-018-21004-w [doi]

Brandao, K., Deason-Towne, F., Zhao, X., Perraud, A. L., & Schmitz, C. (2014). TRPM6 kinase activity regulates TRPM7 trafficking and inhibits cellular growth under hypomagnesian conditions. *Cellular and Molecular Life Sciences : CMLS*, 71(24), 4853-4867. doi:10.1007/s00018-014-1647-7 [doi]

Brauchi, S., Krapivinsky, G., Krapivinsky, L., & Clapham, D. E. (2008). TRPM7 facilitates cholinergic vesicle fusion with the plasma membrane. *Proceedings of the National Academy of Sciences of the United States of America*, 105(24), 8304-8308. doi:10.1073/pnas.0800881105 [doi]

Burgess, S. J., Maasho, K., Masilamani, M., Narayanan, S., Borrego, F., & Coligan, J. E. (2008). The NKG2D receptor: Immunobiology and clinical implications. *Immunologic Research*, 40(1), 18-34. doi:10.1007/s12026-007-0060-9 [doi]

Cabezas-Bratesco, D., Brauchi, S., Gonzalez-Teuber, V., Steinberg, X., Valencia, I., & Colenso, C. (2015). The different roles of the channel-kinases TRPM6 and TRPM7. *Current Medicinal Chemistry*, 22(25), 2943-2953. doi:CMC-EPUB-68899 [pii]

- Cahalan, M. D., & Chandy, K. G. (2009). The functional network of ion channels in T lymphocytes. *Immunological Reviews*, 231(1), 59-87. doi:10.1111/j.1600-065X.2009.00816.x [doi]
- Cai, N., Bai, Z., Nanda, V., & Runnels, L. W. (2017). Mass spectrometric analysis of TRPM6 and TRPM7 phosphorylation reveals regulatory mechanisms of the channel-kinases. *Scientific Reports*, 7, 42739. doi:10.1038/srep42739 [doi]
- Callera, G. E., He, Y., Yogi, A., Montezano, A. C., Paravicini, T., Yao, G., & Touyz, R. M. (2009). Regulation of the novel Mg²⁺ transporter transient receptor potential melastatin 7 (TRPM7) cation channel by bradykinin in vascular smooth muscle cells. *Journal of Hypertension*, 27(1), 155-166.
- Chaigne-Delalande, B., Li, F. Y., O'Connor, G. M., Lukacs, M. J., Jiang, P., Zheng, L., . . . Lenardo, M. J. (2013). Mg²⁺ regulates cytotoxic functions of NK and CD8 T cells in chronic EBV infection through NKG2D. *Science*, 341(6142), 186-191. doi:10.1126/science.1240094 [doi]
- Chokshi, R., Fruasaha, P., & Kozak, J. A. (2012). 2-aminoethyl diphenyl borinate (2-APB) inhibits TRPM7 channels through an intracellular acidification mechanism. *Channels*, 6(5), 362-369. doi:10.4161/chan.21628 [doi]

- Chokshi, R., Matsushita, M., & Kozak, J. A. (2012a). Detailed examination of Mg^{2+} and pH sensitivity of human TRPM7 channels. *American Journal of Physiology. Cell Physiology*, 302(7), C1004-11. doi:10.1152/ajpcell.00422.2011 [doi]
- Chokshi, R., Matsushita, M., & Kozak, J. A. (2012b). Sensitivity of TRPM7 channels to Mg^{2+} characterized in cell-free patches of Jurkat T lymphocytes. *American Journal of Physiology - Cell Physiology*, 302(11), C1642-51. doi:C-00037-2012 [pii]
- Clark, K., Middelbeek, J., Morrice, N. A., Figdor, C. G., Lasonder, E., & van Leeuwen, F. N. (2008). Massive autophosphorylation of the Ser/Thr-rich domain controls protein kinase activity of TRPM6 and TRPM7. *PloS One*, 3(3), e1876. doi:10.1371/journal.pone.0001876 [doi]
- Dasgupta, A., Sarma, D., & Saikia, U. K. (2012). Hypomagnesemia in type 2 diabetes mellitus. *Indian Journal of Endocrinology and Metabolism*, 16(6), 1000-1003. doi:10.4103/2230-8210.103020 [doi]
- Deason-Towne, F., Perraud, A. L., & Schmitz, C. (2012). Identification of Ser/Thr phosphorylation sites in the C2-domain of phospholipase $C\gamma 2$ (PLC $\gamma 2$) using TRPM7-kinase. *Cellular Signalling*, 24(11), 2070-2075. doi:10.1016/j.cellsig.2012.06.015 [doi]

- Desai, B. N., Krapivinsky, G., Navarro, B., Krapivinsky, L., Carter, B. C., Febvay, S., . . . Clapham, D. E. (2012). Cleavage of TRPM7 releases the kinase domain from the ion channel and regulates its participation in fas-induced apoptosis. *Developmental Cell*, 22(6), 1149-1162. doi:10.1016/j.devcel.2012.04.006 [doi]
- Dorovkov, M. V., Beznosov, S. N., Shah, S., Kotlianskaia, L., & Kostiukova, A. S. (2008). Effect of mutations imitating the phosphorylation by TRPM7 kinase on the function of the N-terminal domain of tropomodulin. *Biofizika*, 53(6), 943-949.
- Duan, J., Li, Z., Li, J., Hulse, R. E., Santa-Cruz, A., Valinsky, W. C., . . . Clapham, D. E. (2018). Structure of the mammalian TRPM7, a magnesium channel required during embryonic development. *Proceedings of the National Academy of Sciences of the United States of America*, 115(35), E8201-E8210. doi:10.1073/pnas.1810719115 [doi]
- El Hentati, F. Z., Gruy, F., Iobagiu, C., & Lambert, C. (2010). Variability of CD3 membrane expression and T cell activation capacity. *Cytometry.Part B, Clinical Cytometry*, 78(2), 105-114. doi:10.1002/cyto.b.20496 [doi]
- Faouzi, M., Kilch, T., Horgen, F. D., Fleig, A., & Penner, R. (2017). The TRPM7 channel kinase regulates store-operated calcium entry. *The Journal of Physiology*, 595(10), 3165-3180. doi:10.1113/JP274006 [doi]

- Feske, S. (2009). ORAI1 and STIM1 deficiency in human and mice: Roles of store-operated Ca^{2+} entry in the immune system and beyond. *Immunological Reviews*, 231(1), 189-209. doi:10.1111/j.1600-065X.2009.00818.x [doi]
- Feske, S., Wulff, H., & Skolnik, E. Y. (2015). Ion channels in innate and adaptive immunity. *Annual Review of Immunology*, 33, 291-353. doi:10.1146/annurev-immunol-032414-112212 [doi]
- Frelin, C., Barbry, P., Vigne, P., Chassande, O., Cragoe, E. J., Jr, & Lazdunski, M. (1988). Amiloride and its analogs as tools to inhibit Na^+ transport via the Na^+ channel, the Na^+/H^+ antiport and the $\text{Na}^+/\text{Ca}^{2+}$ exchanger. *Biochimie*, 70(9), 1285-1290. doi:0300-9084(88)90196-4 [pii]
- Gibson, J. N., Beesetty, P., Sulentic, C., & Kozak, J. A. (2016). Rapid quantification of mitogen-induced blastogenesis in T lymphocytes for identifying immunomodulatory drugs. *Journal of Visualized Experiments : JoVE*, (118). doi(118), 10.3791/55212. doi:10.3791/55212 [doi]
- Gunther, T. (2006). Mechanisms, regulation and pathologic significance of Mg^{2+} efflux from erythrocytes. *Magnesium Research*, 19(3), 190-198.

- Gwack, Y., Feske, S., Srikanth, S., Hogan, P. G., & Rao, A. (2007). Signalling to transcription: Store-operated Ca²⁺ entry and NFAT activation in lymphocytes. *Cell Calcium*, 42(2), 145-156. doi:S0143-4160(07)00079-6 [pii]
- Hennekens, C. H., Albert, C. M., Godfried, S. L., Gaziano, J. M., & Buring, J. E. (1996). Adjunctive drug therapy of acute myocardial infarction--evidence from clinical trials. *The New England Journal of Medicine*, 335(22), 1660-1667. doi:10.1056/NEJM199611283352207 [doi]
- Hofmann, T., Schafer, S., Linseisen, M., Sytik, L., Gudermann, T., & Chubanov, V. (2014). Activation of TRPM7 channels by small molecules under physiological conditions. *Pflügers Archiv : European Journal of Physiology*, 466(12), 2177-2189. doi:10.1007/s00424-014-1488-0 [doi]
- Hogan, P. G. (2017). Calcium-NFAT transcriptional signalling in T cell activation and T cell exhaustion. *Cell Calcium*, 63, 66-69. doi:10.1016/j.ceca.2017.01.014 [doi]
- Hogan, P. G., Lewis, R. S., & Rao, A. (2010). Molecular basis of calcium signaling in lymphocytes: STIM and ORAI. *Annual Review of Immunology*, 28, 491-533. doi:10.1146/annurev.immunol.021908.132550 [doi]
- Hou, P., Zhang, R., Liu, Y., Feng, J., Wang, W., Wu, Y., & Ding, J. (2014). Physiological role of Kv1.3 channel in T lymphocyte cell investigated quantitatively

by kinetic modeling. *PLoS One*, 9(3), e89975. doi:10.1371/journal.pone.0089975
[doi]

Huang, C. L., & Kuo, E. (2007). Mechanism of hypokalemia in magnesium deficiency. *Journal of the American Society of Nephrology : JASN*, 18(10), 2649-2652. doi:ASN.2007070792 [pii]

Imboden, J. B., Weiss, A., & Stobo, J. D. (1985). The antigen receptor on a human T cell line initiates activation by increasing cytoplasmic free calcium. *Journal of Immunology*, 134(2), 663-665.

Jahnen-Dechent, W., & Ketteler, M. (2012). Magnesium basics. *Clinical Kidney Journal*, 5(Suppl 1), i3-i14. doi:10.1093/ndtplus/sfr163 [doi]

Jansen, C., Sahni, J., Suzuki, S., Horgen, F. D., Penner, R., & Fleig, A. (2016). The coiled-coil domain of zebrafish TRPM7 regulates Mg²⁺ nucleotide sensitivity. *Scientific Reports*, 6, 33459. doi:10.1038/srep33459 [doi]

Jiang, J., Li, M., & Yue, L. (2005). Potentiation of TRPM7 inward currents by protons. *The Journal of General Physiology*, 126(2), 137-150. doi:jgp.200409185 [pii]

Jin, J., Desai, B. N., Navarro, B., Donovan, A., Andrews, N. C., & Clapham, D. E. (2008). Deletion of *Trpm7* disrupts embryonic development and thymopoiesis

without altering Mg^{2+} homeostasis. *Science*, 322(5902), 756-760.

doi:10.1126/science.1163493 [doi]

Jin, J., Wu, L. J., Jun, J., Cheng, X., Xu, H., Andrews, N. C., & Clapham, D. E. (2012).

The channel kinase, TRPM7, is required for early embryonic development.

Proceedings of the National Academy of Sciences of the United States of America,

109(5), E225-33. doi:10.1073/pnas.1120033109 [doi]

Khalil, M., Alliger, K., Weidinger, C., Yerinde, C., Wirtz, S., Becker, C., & Engel, M. A.

(2018). Functional role of transient receptor potential channels in immune cells and

epithelia. *Frontiers in Immunology*, 9, 174. doi:10.3389/fimmu.2018.00174 [doi]

Kim, T. Y., Shin, S. K., Song, M. Y., Lee, J. E., & Park, K. S. (2012). Identification of

the phosphorylation sites on intact TRPM7 channels from mammalian cells.

Biochemical and Biophysical Research Communications, 417(3), 1030-1034.

doi:10.1016/j.bbrc.2011.12.085 [doi]

Kiryakova, S., Dencheva-Zarkova, M., & Genova, J. (2014). Effect of amphotericin B

antibiotic on the properties of model lipid membrane. *Journal of Physics:*

Conference Series, 558(- 1), 012027.

Kornreich, B. G. (2007). *The patch clamp technique: Principles and technical*

considerations doi:<https://doi.org/10.1016/j.jvc.2007.02.001>

- Kozak, J. A., & Cahalan, M. D. (2003). MIC channels are inhibited by internal divalent cations but not ATP. *Biophysical Journal*, 84(2 Pt 1), 922-927. doi:S0006-3495(03)74909-1 [pii]
- Kozak, J. A., Kerschbaum, H. H., & Cahalan, M. D. (2002). Distinct properties of CRAC and MIC channels in RBL cells. *The Journal of General Physiology*, 120(2), 221-235.
- Kozak, J. A., Matsushita, M., Nairn, A. C., & Cahalan, M. D. (2005). Charge screening by internal pH and polyvalent cations as a mechanism for activation, inhibition, and rundown of TRPM7/MIC channels. *The Journal of General Physiology*, 126(5), 499-514. doi:jgp.200509324 [pii]
- Krapivinsky, G., Krapivinsky, L., Manasian, Y., & Clapham, D. E. (2014). The TRPM7 channel is cleaved to release a chromatin-modifying kinase. *Cell*, 157(5), 1061-1072. doi:10.1016/j.cell.2014.03.046 [doi]
- Krapivinsky, G., Mochida, S., Krapivinsky, L., Cibulsky, S. M., & Clapham, D. E. (2006). The TRPM7 ion channel functions in cholinergic synaptic vesicles and affects transmitter release. *Neuron*, 52(3), 485-496. doi:S0896-6273(06)00771-9 [pii]

- Langeslag, M., Clark, K., Moolenaar, W. H., van Leeuwen, F. N., & Jalink, K. (2007). Activation of TRPM7 channels by phospholipase C-coupled receptor agonists. *The Journal of Biological Chemistry*, 282(1), 232-239. doi:M605300200 [pii]
- Lanier, L. L. (2015). NKG2D receptor and its ligands in host defense. *Cancer Immunology Research*, 3(6), 575-582. doi:10.1158/2326-6066.CIR-15-0098 [doi]
- Laursen, M., Bublitz, M., Moncoq, K., Olesen, C., MÅller, J. V., Young, H. S., . . . Morth, J. P. (2009). Cyclopiazonic acid is complexed to a divalent metal ion when bound to the sarcoplasmic reticulum Ca²⁺-ATPase. *The Journal of Biological Chemistry*, 284(20), 13513-13518. doi:10.1074/jbc.C900031200 [doi]
- Li, F. Y., Chaigne-Delalande, B., Kanellopoulou, C., Davis, J. C., Matthews, H. F., Douek, D. C., . . . Lenardo, M. J. (2011). Second messenger role for Mg²⁺ revealed by human T-cell immunodeficiency. *Nature*, 475(7357), 471-476. doi:10.1038/nature10246 [doi]
- Li, M., Jiang, J., & Yue, L. (2006). Functional characterization of homo- and heteromeric channel kinases TRPM6 and TRPM7. *The Journal of General Physiology*, 127(5), 525-537. doi:jgp.200609502 [pii]
- Lioudyno, M. I., Kozak, J. A., Penna, A., Safrina, O., Zhang, S. L., Sen, D., . . . Cahalan, M. D. (2008). Orai1 and STIM1 move to the immunological synapse and are up-

regulated during T cell activation. *Proceedings of the National Academy of Sciences of the United States of America*, 105(6), 2011-2016. doi:10.1073/pnas.0706122105

[doi]

Lippiat, J. D. (2008). Whole-cell recording using the perforated patch clamp technique. *Methods in Molecular Biology*, 491, 141-149. doi:10.1007/978-1-59745-526-8_11

[doi]

Liu, C., & Hermann, T. E. (1978). Characterization of ionomycin as a calcium ionophore. *The Journal of Biological Chemistry*, 253(17), 5892-5894.

Long, S., & Romani, A. M. (2014). Role of cellular magnesium in human diseases.

Austin Journal of Nutrition and Food Sciences, 2(10) doi:1051

Macianskiene, R., Almanaityte, M., Jekabsone, A., & Mubagwa, K. (2017). Modulation of human cardiac TRPM7 current by extracellular acidic pH depends upon extracellular concentrations of divalent cations. *PloS One*, 12(1), e0170923.

doi:10.1371/journal.pone.0170923 [doi]

Masereel, B., Pochet, L., & Laeckmann, D. (2003). An overview of inhibitors of Na⁺/H⁺ exchanger. *European Journal of Medicinal Chemistry*, 38(6), 547-554.

doi:S0223523403001004 [pii]

- Matsushita, M., Kozak, J. A., Shimizu, Y., McLachlin, D. T., Yamaguchi, H., Wei, F. Y., . . . Nairn, A. C. (2005). Channel function is dissociated from the intrinsic kinase activity and autophosphorylation of TRPM7/ChaK1. *The Journal of Biological Chemistry*, 280(21), 20793-20803. doi:M413671200 [pii]
- Middelbeek, J., Clark, K., Venselaar, H., Huynen, M. A., & van Leeuwen, F. N. (2010). The alpha-kinase family: An exceptional branch on the protein kinase tree. *Cellular and Molecular Life Sciences : CMLS*, 67(6), 875-890. doi:10.1007/s00018-009-0215-z [doi]
- Monteilh-Zoller, M. K., Hermosura, M. C., Nadler, M. J., Scharenberg, A. M., Penner, R., & Fleig, A. (2003). TRPM7 provides an ion channel mechanism for cellular entry of trace metal ions. *The Journal of General Physiology*, 121(1), 49-60.
- Nadolni, W., & Zierler, S. (2018). The channel-kinase TRPM7 as novel regulator of immune system homeostasis. *Cells*, 7(8), 10.3390/cells7080109. doi:E109 [pii]
- Numata, T., & Okada, Y. (2008). Proton conductivity through the human TRPM7 channel and its molecular determinants. *The Journal of Biological Chemistry*, 283(22), 15097-15103. doi:10.1074/jbc.M709261200 [doi]
- Numata, T., Shimizu, T., & Okada, Y. (2007). Direct mechano-stress sensitivity of TRPM7 channel. *Cellular Physiology and Biochemistry : International Journal of*

Experimental Cellular Physiology, Biochemistry, and Pharmacology, 19(1-4), 1-8.

doi:000099187 [pii]

Oancea, E., Wolfe, J. T., & Clapham, D. E. (2006). Functional TRPM7 channels accumulate at the plasma membrane in response to fluid flow. *Circulation Research*, 98(2), 245-253. doi:01.RES.0000200179.29375.cc [pii]

Ogata, K., Tsumuraya, T., Oka, K., Shin, M., Okamoto, F., Kajiya, H., . . . Okabe, K. (2017). The crucial role of the TRPM7 kinase domain in the early stage of amelogenesis. *Scientific Reports*, 7(1), 18099-017-18291-0. doi:10.1038/s41598-017-18291-0 [doi]

Paredes, R. M., Etzler, J. C., Watts, L. T., Zheng, W., & Lechleiter, J. D. (2008). Chemical calcium indicators. *Methods*, 46(3), 143-151. doi:10.1016/j.ymeth.2008.09.025 [doi]

Pegoraro, S., Lang, M., Dreker, T., Kraus, J., Hamm, S., Meere, C., . . . Grissmer, S. (2009). Inhibitors of potassium channels Kv1.3 and IK-1 as immunosuppressants. *Bioorganic & Medicinal Chemistry Letters*, 19(8), 2299-2304. doi:10.1016/j.bmcl.2009.02.077 [doi]

Perraud, A. L., Zhao, X., Ryazanov, A. G., & Schmitz, C. (2011). The channel-kinase TRPM7 regulates phosphorylation of the translational factor eEF2 via eEF2-k. *Cellular Signalling*, 23(3), 586-593. doi:10.1016/j.cellsig.2010.11.011 [doi]

Petkov, G. V. (2009). Chapter 16 - ion channels. In M. Hacker, W. Messer & K. Bachmann (Eds.), *Pharmacology* (pp. 387-427). San Diego: Academic Press. doi:<https://doi.org/10.1016/B978-0-12-369521-5.00016-6> Retrieved from <http://www.sciencedirect.com/science/article/pii/B9780123695215000166>

Ramsey, I. S., Delling, M., & Clapham, D. E. (2006). An introduction to TRP channels. *Annual Review of Physiology*, 68, 619-647. doi:10.1146/annurev.physiol.68.040204.100431 [doi]

Ran, F. A., Hsu, P. D., Wright, J., Agarwala, V., Scott, D. A., & Zhang, F. (2013). Genome engineering using the CRISPR-Cas9 system. *Nature Protocols*, 8(11), 2281-2308. doi:10.1038/nprot.2013.143 [doi]

Raulet, D. H., Gasser, S., Gowen, B. G., Deng, W., & Jung, H. (2013). Regulation of ligands for the NKG2D activating receptor. *Annual Review of Immunology*, 31, 413-441. doi:10.1146/annurev-immunol-032712-095951 [doi]

- Ravell, J., Chaigne-Delalande, B., & Lenardo, M. (2014). Xmen disease: A combined immune deficiency with magnesium defect. *Current Opinion in Pediatrics*, 26(6), 713-719. doi:10.1097/MOP.0000000000000156 [doi]
- Rohacs, T., Lopes, C. M., Michailidis, I., & Logothetis, D. E. (2005). PI(4,5)P₂ regulates the activation and desensitization of TRPM8 channels through the TRP domain. *Nature Neuroscience*, 8(5), 626-634. doi:nn1451 [pii]
- Romani, A. M. (2011). Cellular magnesium homeostasis. *Archives of Biochemistry and Biophysics*, 512(1), 1-23. doi:10.1016/j.abb.2011.05.010 [doi]
- Roos, J., DiGregorio, P. J., Yeromin, A. V., Ohlsen, K., Liudyno, M., Zhang, S., . . . Stauderman, K. A. (2005). STIM1, an essential and conserved component of store-operated Ca²⁺ channel function. *The Journal of Cell Biology*, 169(3), 435-445. doi:jcb.200502019 [pii]
- Rosanoff, A., Weaver, C. M., & Rude, R. K. (2012). Suboptimal magnesium status in the united states: Are the health consequences underestimated? *Nutrition Reviews*, 70(3), 153-164. doi:10.1111/j.1753-4887.2011.00465.x [doi]
- Rude, R. K., Gruber, H. E., Wei, L. Y., Frausto, A., & Mills, B. G. (2003). Magnesium deficiency: Effect on bone and mineral metabolism in the mouse. *Calcified Tissue International*, 72(1), 32-41. doi:10.1007/s00223-001-1091-1 [doi]

- Runnels, L. W., Yue, L., & Clapham, D. E. (2002). The TRPM7 channel is inactivated by PIP₂ hydrolysis. *Nature Cell Biology*, 4(5), 329-336. doi:10.1038/ncb781 [doi]
- Ryan, M. P. (1993). Interrelationships of magnesium and potassium homeostasis. *Mineral and Electrolyte Metabolism*, 19(4-5), 290-295.
- Ryazanov, A. G. (2002). Elongation factor-2 kinase and its newly discovered relatives. *FEBS Letters*, 514(1), 26-29. doi:S0014579302022998 [pii]
- Ryazanova, L. V., Rondon, L. J., Zierler, S., Hu, Z., Galli, J., Yamaguchi, T. P., . . . Ryazanov, A. G. (2010). TRPM7 is essential for Mg²⁺ homeostasis in mammals. *Nature Communications*, 1, 109. doi:10.1038/ncomms1108 [doi]
- Sah, R., Mesirca, P., Mason, X., Gibson, W., Bates-Withers, C., Van den Boogert, M., . . . Clapham, D. E. (2013). Timing of myocardial trpm7 deletion during cardiogenesis variably disrupts adult ventricular function, conduction, and repolarization. *Circulation*, 128(2), 101-114. doi:10.1161/CIRCULATIONAHA.112.000768 [doi]
- Sah, R., Mesirca, P., Van den Boogert, M., Rosen, J., Mably, J., Mangoni, M. E., & Clapham, D. E. (2013). Ion channel-kinase TRPM7 is required for maintaining cardiac automaticity. *Proceedings of the National Academy of Sciences of the United States of America*, 110(32), E3037-46. doi:10.1073/pnas.1311865110 [doi]

- Sahni, J., & Scharenberg, A. M. (2008). TRPM7 ion channels are required for sustained phosphoinositide 3-kinase signaling in lymphocytes. *Cell Metabolism*, 8(1), 84-93. doi:10.1016/j.cmet.2008.06.002 [doi]
- Sahni, J., Tamura, R., Sweet, I. R., & Scharenberg, A. M. (2010). TRPM7 regulates quiescent/proliferative metabolic transitions in lymphocytes. *Cell Cycle*, 9(17), 3565-3574. doi:10.4161/cc.9.17.12798 [doi]
- Schlingmann, K. P., Weber, S., Peters, M., Niemann Nejsum, L., Vitzthum, H., Klingel, K., . . . Konrad, M. (2002). Hypomagnesemia with secondary hypocalcemia is caused by mutations in TRPM6, a new member of the TRPM gene family. *Nature Genetics*, 31(2), 166-170. doi:10.1038/ng889 [doi]
- Smith-Garvin, J. E., Koretzky, G. A., & Jordan, M. S. (2009). T cell activation. *Annual Review of Immunology*, 27, 591-619. doi:10.1146/annurev.immunol.021908.132706 [doi]
- Standley, P. R., & Standley, C. A. (2002). Identification of a functional Na⁺/Mg²⁺ exchanger in human trophoblast cells. *American Journal of Hypertension*, 15(6), 565-570. doi:S0895706102022720 [pii]
- Stritt, S., Nurden, P., Favier, R., Favier, M., Ferioli, S., Gotru, S. K., . . . Braun, A. (2016). Defects in TRPM7 channel function deregulate thrombopoiesis through

- altered cellular Mg^{2+} homeostasis and cytoskeletal architecture. *Nature Communications*, 7, 11097. doi:10.1038/ncomms11097 [doi]
- Swaminathan, R. (2003). Magnesium metabolism and its disorders. *The Clinical Biochemist.Reviews*, 24(2), 47-66.
- Trebak, M., & Kinet, J. P. (2019). Calcium signalling in T cells. *Nature Reviews.Immunology*, 19(3), 154-169. doi:10.1038/s41577-018-0110-7 [doi]
- Vaeth, M., & Feske, S. (2018). Ion channelopathies of the immune system. *Current Opinion in Immunology*, 52, 39-50. doi:10.1016/j.coi.2018.03.021 [doi]
- Venkatachalam, K., & Montell, C. (2007). TRP channels. *Annual Review of Biochemistry*, 76, 387-417. doi:10.1146/annurev.biochem.75.103004.142819 [doi]
- Verheugen, J. A., Vijverberg, H. P., Oortgiesen, M., & Cahalan, M. D. (1995). Voltage-gated and Ca^{2+} -activated K^{+} channels in intact human T lymphocytes. noninvasive measurements of membrane currents, membrane potential, and intracellular calcium. *The Journal of General Physiology*, 105(6), 765-794. doi:10.1085/jgp.105.6.765 [doi]
- Verneris, M. R., Karimi, M., Baker, J., Jayaswal, A., & Negrin, R. S. (2004). Role of NKG2D signaling in the cytotoxicity of activated and expanded $CD8^{+}$ T cells. *Blood*, 103(8), 3065-3072. doi:10.1182/blood-2003-06-2125 [doi]

- Viering, D. H. H. M., de Baaij, J. H. F., Walsh, S. B., Kleta, R., & Bockenhauer, D. (2017). Genetic causes of hypomagnesemia, a clinical overview. *Pediatric Nephrology*, 32(7), 1123-1135. doi:10.1007/s00467-016-3416-3 [doi]
- Visser, D., Middelbeek, J., van Leeuwen, F. N., & Jalink, K. (2014). Function and regulation of the channel-kinase TRPM7 in health and disease. *European Journal of Cell Biology*, 93(10-12), 455-465. doi:10.1016/j.ejcb.2014.07.001 [doi]
- Voets, T., Nilius, B., Hoefs, S., van der Kemp, A. W., Droogmans, G., Bindels, R. J., & Hoenderop, J. G. (2004). TRPM6 forms the Mg²⁺ influx channel involved in intestinal and renal Mg²⁺ absorption. *The Journal of Biological Chemistry*, 279(1), 19-25. doi:10.1074/jbc.M311201200 [doi]
- Walder, R. Y., Landau, D., Meyer, P., Shalev, H., Tsolia, M., Borochowitz, Z., . . . Sheffield, V. C. (2002). Mutation of TRPM6 causes familial hypomagnesemia with secondary hypocalcemia. *Nature Genetics*, 31(2), 171-174. doi:10.1038/ng901 [doi]
- Wei, C., Wang, X., Chen, M., Ouyang, K., Song, L. S., & Cheng, H. (2009). Calcium flickers steer cell migration. *Nature*, 457(7231), 901-905. doi:10.1038/nature07577 [doi]

- Wickenden, A. D. (2014). Overview of electrophysiological techniques. *Current Protocols in Pharmacology*, 64, 11.1.1-17. doi:10.1002/0471141755.ph1101s64 [doi]
- Wiemann, K., Mittrucker, H. W., Feger, U., Welte, S. A., Yokoyama, W. M., Spies, T., . . . Steinle, A. (2005). Systemic NKG2D down-regulation impairs NK and CD8 T cell responses in vivo. *Journal of Immunology*, 175(2), 720-729. doi:175/2/720 [pii]
- Xie, J., Sun, B., Du, J., Yang, W., Chen, H. C., Overton, J. D., . . . Yue, L. (2011). Phosphatidylinositol 4,5-bisphosphate (PIP₂) controls magnesium gatekeeper TRPM6 activity. *Scientific Reports*, 1, 146. doi:10.1038/srep00146 [doi]
- Yamaguchi, H., Matsushita, M., Nairn, A. C., & Kuriyan, J. (2001). Crystal structure of the atypical protein kinase domain of a TRP channel with phosphotransferase activity. *Molecular Cell*, 7(5), 1047-1057. doi:S1097-2765(01)00256-8 [pii]
- Yee, N. S., Kazi, A. A., & Yee, R. K. (2014). Cellular and developmental biology of TRPM7 channel-kinase: Implicated roles in cancer. *Cells*, 3(3), 751-777. doi:10.3390/cells3030751 [doi]
- Zhelay, T., Wiczerzak, K. B., Beesetty, P., Alter, G. M., Matsushita, M., & Kozak, J. A. (2018). Depletion of plasma membrane-associated phosphoinositides mimics

inhibition of TRPM7 channels by cytosolic Mg^{2+} , spermine, and pH. *The Journal of Biological Chemistry*, 293(47), 18151-18167. doi:10.1074/jbc.RA118.004066 [doi]

Zhou, H., & Clapham, D. E. (2009). Mammalian MagT1 and TUSC3 are required for cellular magnesium uptake and vertebrate embryonic development. *Proceedings of the National Academy of Sciences of the United States of America*, 106(37), 15750-15755. doi:10.1073/pnas.0908332106 [doi]